The Journal of Comparative Neurology 517:459–480 (2009)
Research in Systems Neuroscience

Morphology of Retinal Ganglion Cells in the Ferret (*Mustela putorius furo*)

TOMOKI ISAYAMA,[1,2] BRENDAN J. O'BRIEN,[1,3]* IRMA UGALDE,[1] JAY F. MULLER,[1] AARON FRENZ,[1] VIKAS AURORA,[1] WILLIAM TSIARAS,[1] AND DAVID M. BERSON[1]

[1]Department of Neuroscience, Brown University, Providence, Rhode Island 02912
[2]Department of Ophthalmology, Massachusetts Eye and Ear Infirmary, Harvard Medical School, Boston, Massachusetts 02114
[3]Visual Sciences Group, Research School of Biology and Department of Psychology, Australian National University, Canberra, Australian Capital Territory 2600, Australia

ABSTRACT

The ferret is the premiere mammalian model of retinal and visual system development, but the spectrum and properties of its retinal ganglion cells are less well understood than in another member of the Carnivora, the domestic cat. Here, we have extensively surveyed the dendritic architecture of ferret ganglion cells and report that the classification scheme previously developed for cat ganglion cells can be applied with few modifications to the ferret retina. We confirm the presence of alpha and beta cells in ferret retina, which are very similar to those in cat retina. Both cell types exhibited an increase in dendritic field size with distance from the area centralis (eccentricity) and with distance from the visual streak. Both alpha and beta cell populations existed as two subtypes whose dendrites stratified mainly in sublamina a or b of the inner plexiform layer. Six additional morphological types of ganglion cells were identified: four monostratified cell types (delta, epsilon, zeta, and eta) and two bistratified types (theta and iota). These types closely resembled their counterparts in the cat in terms of form, relative field size, and stratification. Our data indicate that, among carnivore species, the retinal ganglion cells resemble one another closely and that the ferret is a useful model for studies of the ontogenetic differentiation of ganglion cell types. J. Comp. Neurol. 517:459–480, 2009.

Indexing terms: carnivores; topography; dye filling; area centralis; visual streak; stratification; taxonomy

Ganglion cells are the output neurons of the retina, providing the channel through which information is transmitted from the retina to central visual areas. Recent work suggests that mammalian retinas possess more than a dozen anatomically distinct types of retinal ganglion cells (Kolb et al., 1981, 1992; Amthor et al., 1989; Peichl, 1989; Watanabe and Rodieck, 1989; Rodieck and Watanabe, 1993; Sun et al., 2002a,b; Kong et al., 2005; Coombs et al., 2006). These types are distinguished by unique patterns of central projection, retinal distribution, dendritic arborization, and synaptic affiliation in the inner plexiform layer (IPL). Each type appears to establish a characteristic mosaic, with somata arranged in a quasiregular lattice and dendritic fields minimally overlapping such that they efficiently tile the retinal surface (for review see Wässle and Boycott, 1991).

A central challenge for retinal biologists is to understand the developmental mechanisms driving the differentiation of these neuronal cell types. An attractive model for such studies is the ferret, which by comparison with other mammals has an immature visual system at birth (Jackson and Hickey, 1985; Henderson et al., 1988; Reese and Urich, 1994). Many events critical to shaping ganglion cell form and function occur postnatally in the ferret. These include specification of the size of the ganglion cell population; the emergence of topographic variations in cell density, synaptogenesis, and sublaminar specialization within the IPL; dendritic outgrowth and remodeling; and axonal target refinement (Greiner and Weidman, 1981; Vitek et al., 1985; Maslim and Stone, 1986, 1988; Henderson et al., 1988; Penn et al., 1994, 1998; Bodnarenko et al., 1995, 1999; Wingate and Thompson, 1995; Lohmann and Wong, 2001; Stellwagen and Shatz, 2002).

The central goal of the present study is to lay the foundation for future developmental studies of ferret retina by providing a more complete accounting of its ganglion cell types. Earlier

Grant sponsor: National Eye Institute; Grant number: EY06108 (to D.M.B.); Grant sponsor: National Institutes of Health; Grant number: MH19118-06 (to B.J.O.).

*Correspondence to: Brendan J. O'Brien, Visual Sciences Group, Research School of Biology and Department of Psychology, Australian National University, Canberra, ACT 2600, Australia.
E-mail: b.obrien@anu.edu.au

Received 18 January 2009; Revised 17 May 2009; Accepted 4 July 2009
DOI 10.1002/cne.22145
Published online July 16, 2009 in Wiley InterScience (www.interscience.wiley.com).

work has established the existence of alpha and beta cells closely resembling their counterparts in cat retina and has outlined their distribution, relative frequency, and central projections (Henderson, 1985; Vitek et al., 1985; Amthor and Jackson, 1986; Wingate et al., 1992). Both of these types have also been shown to comprise OFF and ON varieties, arborizing, respectively, in sublamina a and b of the IPL (Kageyama and Wong-Riley, 1984; Peichl et al., 1987a; Wingate et al., 1992), although stratification has yet to be analyzed quantitatively. In at least one important respect, however, ferret alpha and beta cells may differ markedly from those in cats: their dendritic fields have been reported to exhibit no systematic variation in size as a function of retinal location or ganglion cell density (Wingate et al., 1992; but see also Vitek et al., 1985; Peichl et al., 1987a). This raises the possibility that factors and principles governing ganglion cell dendritic development may be idiosyncratic in the ferret retina, limiting its utility as a general model of ganglion cell development.

A second set of unresolved issues concerns the diverse population of ferret ganglion cells that are neither alpha nor beta cells. Several provisional types or groups have been identified within this population (Vitek et al., 1985; Wingate et al., 1992), but a formal taxonomy has not been advanced. Substantial progress has been made, however, in the formal classification of ganglion cell types in the retina of cats (Boycott and Wässle, 1974; Leventhal et al., 1980; Kolb et al., 1981; Famiglietti, 1987; Dacey, 1989; Pu et al., 1994; Stein et al., 1996; Berson et al., 1998, 1999a,b; Isayama et al., 1999, 2000; O'Brien et al., 2002), which belong to the same taxonomic order as ferrets and share with them many aspects of retinal organization (Weidman and Greiner, 1984; Jackson and Hickey, 1985). We were interested in the possibility that the cat classification scheme might provide a useful framework for classifying ferret ganglion cells.

Here we report findings based on a large sample of ferret ganglion cells stained by intracellular dye injection in vitro. This study provides new details regarding the stratification and topography of ferret alpha and beta cells and demonstrates the existence of at least six other ferret ganglion cell types, each with an easily recognized counterpart in cat retina.

MATERIALS AND METHODS

Intracellular staining

Methods were similar to those we have used for staining cat ganglion cells in vitro, as described in detail elsewhere (Pu and Berson, 1992; Pu et al., 1994; Berson et al., 1998, 1999b; Isayama et al., 2000). All procedures were approved by the Brown University Institutional Animal Care and Use Committee. In short, eyes were enucleated from adult female pigmented ferrets >20 weeks old (n = 48) under deep barbiturate anesthesia (Nembutal, 25 mg/kg). Afterward, the animals were killed with an overdose of Nembutal. The globe was hemisected just behind the limbus, and the lens and vitreous were removed. Several relieving cuts were made, and the tissue was mounted on filter paper (MSI, Westboro, MA) vitreal side up, either as a flattened eyecup or after isolation of the retina from the other layers of the globe. The tissue was placed in a chamber on a fixed-stage epifluorescence microscope (Olympus Corporation, Lake Success, NY) and superfused at approximately 4 ml/min with Ames' medium supplemented with 10 mM dextrose (pH 7.4; Sigma, St. Louis, MO) at room temperature.

Ganglion cell bodies were stained by adding to the bath a small amount of the vital dye acridine orange (50–100 μl of a 100 μg/ml solution in Ames' medium). Micropipettes (tip diameters <1 μm; 100–300 MΩ) contained 4% Lucifer yellow CH (LY; Sigma) and 4% biocytin (Molecular Probes, Eugene, OR) in 0.05 M Tris buffer (pH 7.4) and had DC resistances of 50–200 MΩ. The pipette was advanced with a micromanipulator (Leitz) onto a labeled soma while viewing both tip and cell with a ×40 water-immersion lens (Nikon, Garden City, NY). Cells were impaled by delivering very brief pulses of oscillation (capacitance overcompensation) or of voltage with an intracellular amplifier (Cygnus Technology, Inc., Delaware Gap, PA). Care was taken to keep the intensity and duration of the pulses as low as possible to avoid damage to the cell. Dyes were injected into the cell for several minutes with biphasic current pulses (up to −4 nA and +0.5 nA). As many as 50 cells were filled in each retina over periods lasting approximately 8 hours.

Retinas were fixed for 2 hours (4.0% paraformaldehyde in 0.1 M phosphate-buffered saline, pH 7.4), processed immunocytochemically for LY and biocytin (Pu and Berson, 1992), mounted on glass slides, and coverslipped with 60% glycerol in phosphate buffer. To minimize shrinkage in retinal thickness and facilitate the analysis of dendritic stratification, the retinas were neither dehydrated nor cleared. The resulting sacrifice in optical resolution was modest, so even thin processes were easily traced to abrupt endings.

Labeled cells were examined under brightfield microscopy. The positions of the area centralis and visual streak were identified from an examination of the density of cells in the ganglion cell layer (GCL), visible from nonspecific histochemical staining or by oblique illumination. The area centralis, the region of peak ganglion cell density, lies approximately 2.5 mm temporal to the optic disk. The visual streak is a horizontal band of elevated ganglion cell density in the nasal retina that grazes the optic disk and intersects the area centralis (Henderson, 1985; Vitek et al., 1985). By using a digital morphometry system (Neurolucida; MicroBrightField, Colchester, VT), we measured each cell's eccentricity (defined as its linear distance from the area centralis) and its minimum distance from the axis of the visual streak.

Dendritic-field dimensions were measured only in cells with complete filling of their distal dendrites. We used NeuroLucida to determine the area of a convex polygon minimally encompassing the cell's dendritic profile (i.e., with its vertices at the tips of the most peripheral processes) and calculated the equivalent diameter (diameter of a circle equal in area to this polygon). Soma diameters were taken to be the average of the maximum and minimum diameter as measured with an eyepiece graticule. For the photomicrographs of Figure 5, cells were photographed with a green interference filter and T-Max 100 film. Negatives were digitally scanned (Nikon Coolscan) and then processed and printed in Photoshop (Adobe Systems, Inc.). Only globally applied filters (e.g., adjust levels) were used on each image.

Analysis of stratification

Depth of dendritic stratification was assessed by through-focus observation in retinal wholemounts using brightfield

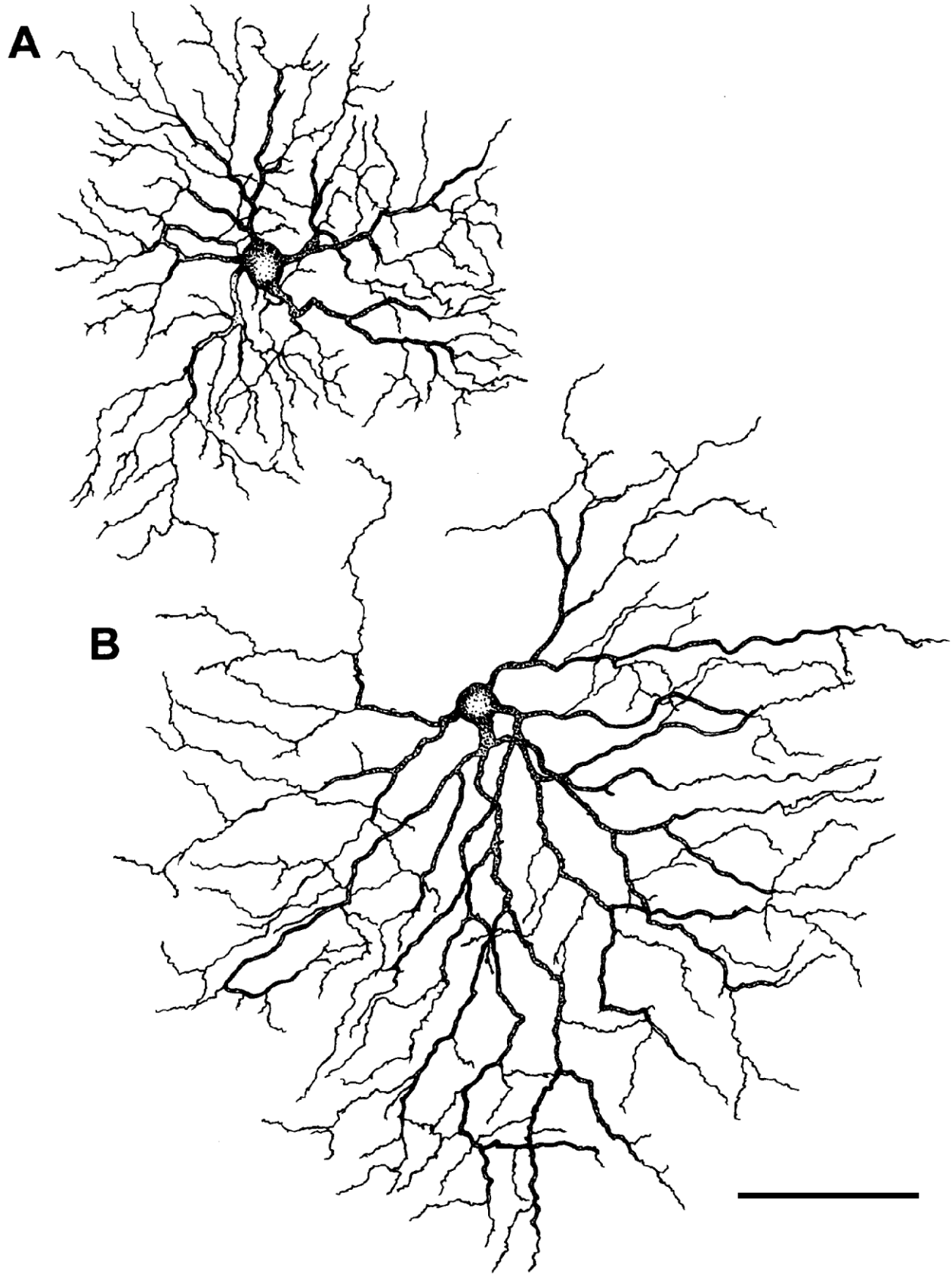

Figure 1.
Camera lucida drawings of representative alpha cells of the ferret retina stained by intracellular injection. Both cells had filled axons, but these have been omitted for clarity. Distance from the area centralis, or eccentricity (e), and distance from the axis of the visual streak (s) as follows. **A:** e = +0.7 mm; s = +0.7 mm; **B:** e = +5.7 mm; s = +1.4 mm. Negative values of e indicate locations in temporal hemiretina; negative values of s indicate locations in inferior retina. Scale bar = 100 μm.

optics and a ×60 objective lens with a correction collar (numerical aperture 0.85, working distance 0.43). The limits of the IPL were inferred from the depth of somata in the GCL and of the innermost cell bodies of the inner nuclear layer (INL), visible from nonspecific histochemical staining or by oblique illumination. The depth of the outer border of the IPL could be estimated more precisely (typically ±1–2 μm) than the inner border (±3–4 μm), because the cell density was higher and the soma smaller and more uniform in the INL than in the GCL. For 113 cells, mutual overlap of dendritic fields with one or more other cells permitted through-focus assessment of the relative depth of dendritic stratification of different types. For four cells, we quantified the differences in depth with NeuroLucida. Depth measurements were corrected according to Snell's law as described elsewhere (Berson et al., 1998).

For 10 alpha and beta cells, we analyzed dendritic stratification quantitatively in radial sections. Cells selected for study were filled optimally and were well isolated from other stained elements. Cells were drawn with a camera lucida, excised with a dermal punch (Acuderm, Ft. Lauderdale, FL), dehydrated in graded ethanols, and embedded in plastic (Poly/Bed 812 resin; Polysciences, Warrington, PA). Radial sections of ~20-μm thickness were cut on a sliding microtome, mounted on glass slides, coverslipped with plastic film and fresh epoxy resin, and cured. We restricted study to the periphery of the dendritic field, so low order dendrites ascending to the main layer of arborization were excluded from the analysis. Camera lucida drawings were made of stained processes and of somatic profiles in the INL and GCL, which were visible from background staining. Within each section, the depths of dendritic segments were measured at regularly spaced horizontal intervals amounting to one-twentieth of the horizontal extent of the measured process. Depths were expressed as a percentage of the total thickness of the IPL (with 0% corresponding to the scleral boundary and 100% to the vitreal boundary). For stout processes, the middle of the dendrite's thickness was used for such measurements. Typically, 20 sites were analyzed per section for alpha cells and 10–15 sites for beta cells.

RESULTS

Alpha and beta cells

Cells very similar in form to cat alpha and beta cells were easily recognizable among the ferret ganglion cell population, as previously reported (Vitek et al., 1985; Amthor and Jackson, 1986; Peichl et al., 1987a; Wingate et al., 1992). Ferret alpha cells (Fig. 1) had the largest somata (see Fig. 14, Table 1) and thickest axons of all ferret ganglion cells. Their stout dendrites formed a radiate, largely nonoverlapping arbor that was among the largest of all ferret ganglion cell types (270–690 μm in diameter; see Figs. 3A, 13B). Dendrites ramified either in sublamina a (OFF sublayer) or in sublamina b (ON sublayer) of the IPL.

Beta cells (Fig. 2) were intermediate among ferret ganglion cells in cell body size (see Fig. 14, Table 1) and axon caliber. Their bushy dendritic arbors were smaller in diameter than those of any other class of ferret ganglion cell (50–210 μm in diameter; Figs. 3B, 13B). Beta cell arbors ramified broadly either in sublamina a or in sublamina b of the IPL.

Topography of dendritic field size. Alpha and beta cell dendritic fields increased in size as a function of eccentricity (distance from the area centralis; Fig. 3A) and also as a function of their distance from the visual streak (Fig. 3B; see also Figs. 1, 2). In the nasal retina, field size was more closely related to its distance from the streak than it was to eccentricity, accounting for more than twice as much of the variance for both cell types (linear regression analysis, Table 2). This was not true in the temporal retina.

The eccentricity data (Fig. 3A) are replotted in Figure 3C,D using different symbols for distinct ranges of distance from the streak. In the nasal periphery, much of the variability in field size was attributable to the influence of the visual streak. The largest nasal fields lay far from the streak (open circles) and the smallest ones lay near it (solid lozenges). This source of variability did not apply to the central retina, where all cells are, by definition, near the streak. Consequently, the correlation between distance from the streak and field size (Fig. 3B) ensures at least a weak relationship between field size and eccentricity (Fig. 3A). The influence of the visual streak can be factored out by restricting consideration to cells lying very near the streak (solid diamonds in Fig. 3C,D). In the nasal retina, mean field diameter for these cells increased by one-third from the area centralis to the peripheral streak, a trend more apparent for alpha cells (Fig. 3C) than for beta cells (Fig. 3D). For alpha cells, this difference in field size was comparable to that between peripheral streak and peripheral nonstreak retina (compare solid diamonds and open circles in Fig. 3C). For beta cells, by contrast, fields roughly doubled in diameter between streak and nonstreak periphery, about three times as large an increase as that between area centralis and peripheral streak (Fig. 3D).

In the temporal hemiretina, beta cell field diameter was correlated with eccentricity, roughly tripling in size from center to periphery (Fig. 3D). Little if any of this correlation, however, was attributable to the influence of the visual streak. That is, beta cells near the streak were not markedly smaller than those far from the streak at a given temporal eccentricity. This was presumably because the streak is weakly developed in temporal retina (Henderson, 1985). A similar trend was apparent among alpha cells temporally (Fig. 3C), although the sample is small.

Table 2 lists the constants defining the least-squares regression lines shown in Figure 3A,B. The ratio of slope (m) to Y-intercept (b) is a measure of the proportional increase in dendritic field diameter per millimeter of retinal distance. These ratios were substantially higher for beta cells than for alpha cells. They indicate that beta cell dendritic field areas increased about 3.4-fold from the area centralis to the far periphery (7 mm eccentricity), whereas alpha fields increased only 1.7-fold. Similarly, beta cell fields increased in area an average of 7.5-fold from the visual streak to the superior or inferior periphery (6 mm from the streak), whereas alpha cell fields increased only 2.9-fold. If each type's dendritic field area is inversely proportional to its local density (Wässle and Boycott, 1991), this suggests that the ratio of beta cell to alpha cell density should be two or three times higher in the central retina than in the periphery.

Stratification. Ferret alpha and beta cells exhibited patterns of dendritic stratification very similar to their counterparts in cat retina. Each comprised a paramorphic pair of types (Famiglietti and Kolb, 1976) that closely matched one another in somadendritic form but ramified separately in either

TABLE 1. Dendritic Field and Soma Sizes of Ferret Ganglion Cells[1]

	Dendritic field			Soma		
Type	Mean diameter (μm)	SD	n	Mean diameter (μm)	SD	n
Alpha	423	75	154	25.4	3.9	47
Beta	115	34	315	18.2	2.0	39
Delta	327	81	20	15.4	1.7	18
Epsilon	406	92	16	16.3	2.1	14
Zeta	160	36	59	13.7	1.4	59
Eta	195	46	33	14.0	1.3	33
Theta	183	38	71	13.7	1.3	71
Iota	304	53	19	15.4	1.7	19

[1]Samples of individual cell types were similar to one another in topographic distribution (cf. Figs. 3B–D, 13A).

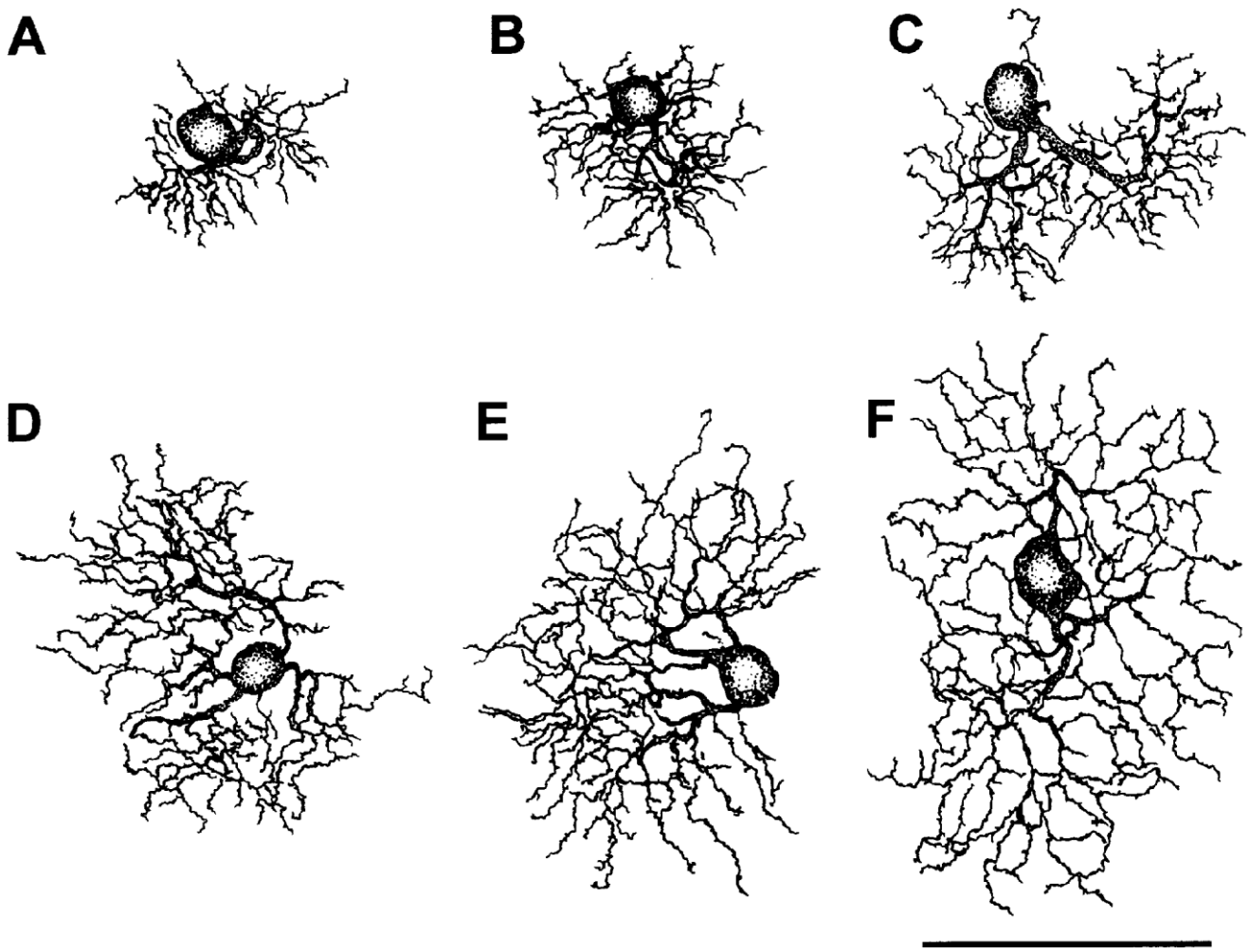

Figure 2.
Camera lucida drawings of beta ganglion cells of the ferret retina. Cells A–C all lay within the nasal visual streak, but at progressively greater eccentricities from left to right. Cells D–F all lay outside the visual streak, with increasing eccentricity and distance from the visual streak from left to right. Axons omitted for clarity. Cell locations as follows (conventions as for Fig. 1): **A:** e = +0.1, s = +0.1; **B:** e = +3.3, s = +0.0; **C:** e = +6.9, s = +0.1; **D:** e = –1.6, s = –0.4; **E:** e = +3.0, s = +3.0; **F:** e = +5.8, s = +4.3. Scale bar = 100 μm.

sublamina a (OFF sublayer) or sublamina b (ON sublayer) of the IPL. Adopting conventions used in cat retina (Wässle and Boycott, 1991), we will refer to these four types as OFF alpha, ON alpha, OFF beta, and ON beta cells. Figure 4A–F illustrates the stratification patterns revealed in radial sections of each type. OFF beta cells ramified throughout sublamina a and ON beta cells in most of sublamina b, sparing only its innermost part (Fig. 4C,D,F). ON and OFF alpha cells costratified extensively with ON and OFF beta cells, respectively, but were more narrowly stratified (Fig. 4E,F).

Analysis of stratification by through-focus examination in wholemounts at points of intersection between overlapping

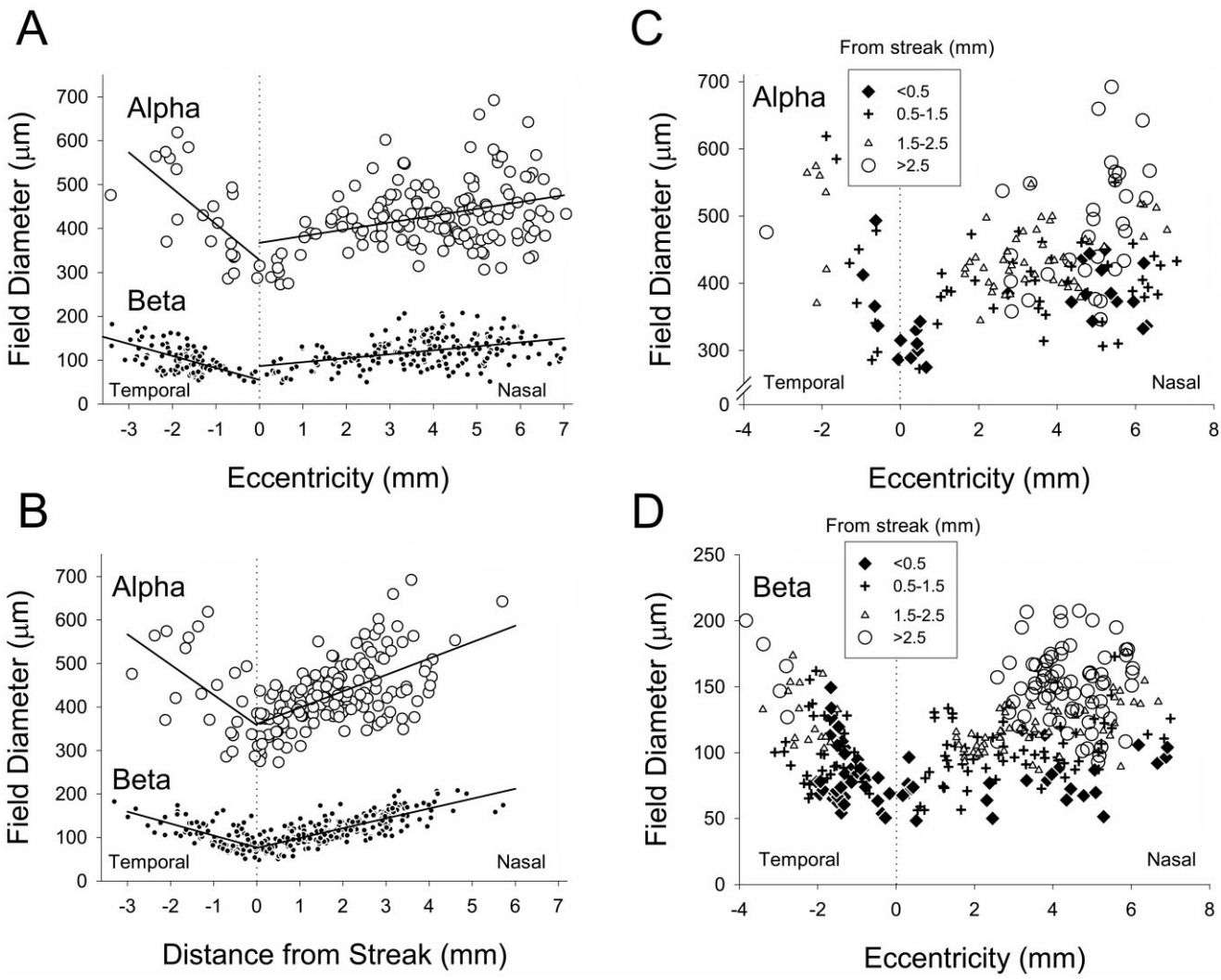

Figure 3.
Topographic dependence of dendritic field size for ferret alpha and beta ganglion cells. **A,B:** Dependence of dendritic field diameter on eccentricity (i.e., distance from the center of the area centralis; A) and distance from the axis of the visual streak (B). No distinction is made in A or in B between superior and inferior hemiretinas. Lines indicate linear least-squares fits to the data. Regression constants shown in Table 2. **C,D:** Plots illustrating relative contribution of eccentricity and distance from the visual streak to dendritic field size of alpha (C) and beta (D) cells. Each symbol type indicates a range of distance from the axis of the visual streak, as indicated in the key. Negative eccentricities lie in the temporal hemiretina.

TABLE 2. Regression Constants for Dendritic Fields as a Function of Eccentricity or Distance From Visual Streak[1]

Cell type	Independent variable	Hemiretina	Slope (m)	Y-intercept (b)	m/b	r^2
Alpha	Eccentricity	Nasal	15.5	367.4	0.04	0.12
Alpha	Eccentricity	Temporal	–81.5	328.5	–0.25	0.41
Beta	Eccentricity	Nasal	9.0	87.1	0.10	0.18
Beta	Eccentricity	Temporal	–27.3	55.4	–0.49	0.41
Alpha	Streak distance	Nasal	37.7	360.9	0.10	0.34
Alpha	Streak distance	Temporal	–69.6	358.4	–0.19	0.28
Beta	Streak distance	Nasal	22.6	76.1	0.30	0.62
Beta	Streak distance	Temporal	–27.3	77.0	–0.35	0.52

[1]Regression constants for least squares fits of Figure 3A,B.

dendritic profiles (Fig. 4G,H) suggested somewhat narrower stratification than indicated by the radial-section data (Fig. 4E,F). Figure 4G compares the relative depth of ramification of three cells with mutually overlapping dendritic fields: an ON alpha, an OFF alpha, and an ON beta cell. For clarity, the depth values were normalized to the depth of the ON alpha dendrites (horizontal dashed line at 0 depth). The OFF alpha cell's dendrites (solid bars) always lay at least several micrometers distal to those of the ON alpha. The ON beta cell's dendrites (stippled bars) spanned a broader depth range than

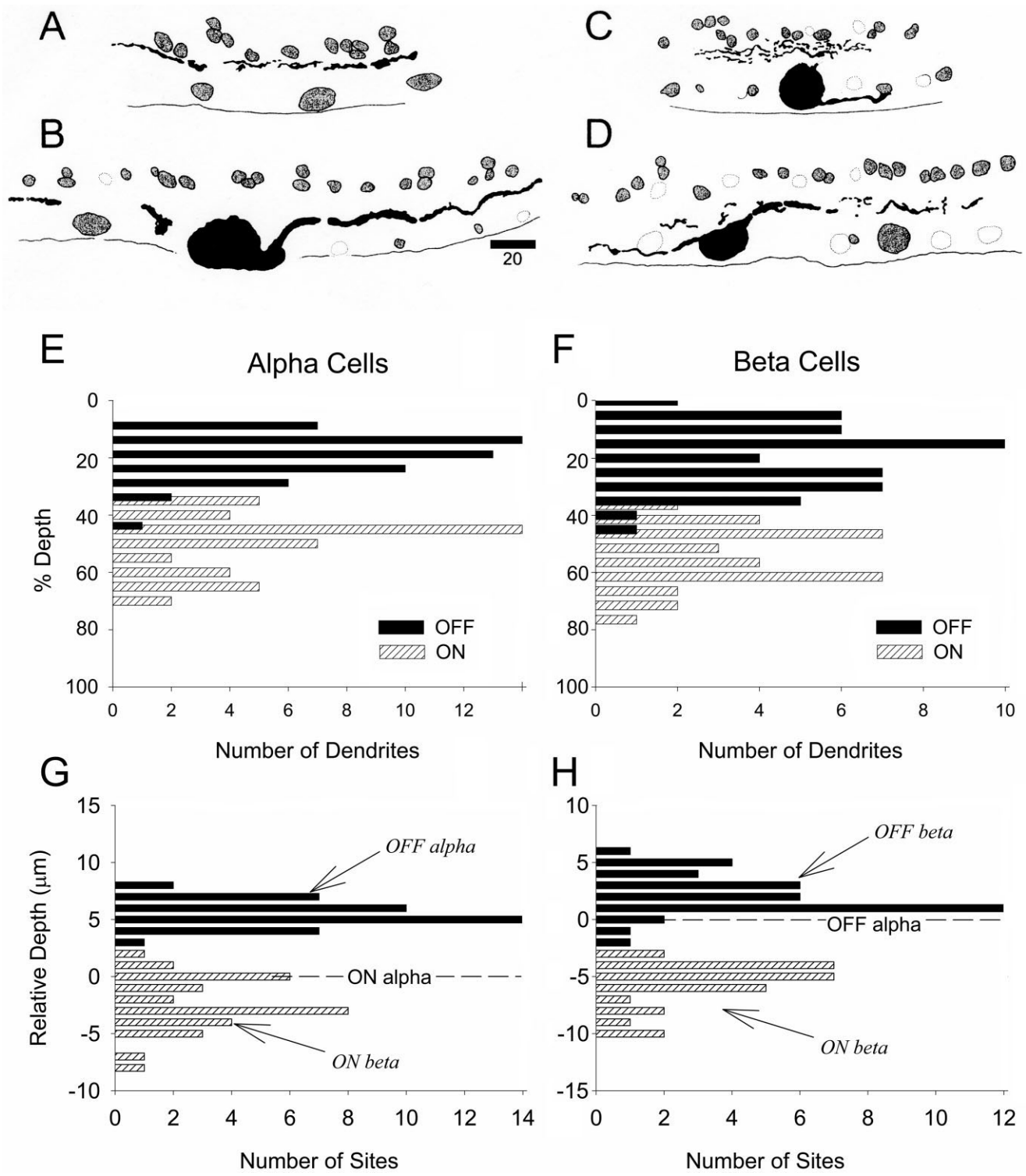

Figure 4.
Depths of dendritic stratification for ferret alpha and beta ganglion cells. **A–D:** Camera lucida drawings of representative radial sections. A: OFF alpha; B: ON alpha; C: OFF beta; D: ON beta. Black somata and processes belong to the injected cell; the soma for the cell in A lies out of the plane of the section illustrated. Shaded profiles represent other cell bodies of the ganglion cell and inner nuclear layers. **E,F:** Histograms of relative frequency of dendritic processes at depths in the inner plexiform layer (IPL), expressed as a percentage of its total thickness; 0% corresponds to the distal border and 100% to the proximal border of the IPL. For both alpha cells (E) and beta cells (F), stippled bars indicate dendrites of ON type, solid bars those of OFF type. Data drawn from one ON alpha, one OFF alpha, three ON beta, and three OFF beta cells. **G,H:** Relative depths of stratification of alpha and beta cells as revealed by quantitative through-focus analysis in a single retinal whole mount of cells with overlapping dendritic profiles. For each panel, a single alpha cell was selected as a reference cell. At each point of intersection between the dendritic profiles of the reference cell and another cell with an overlapping field, the difference in depth between the two dendrites was measured. The histograms plot the distribution of these depth differences. G: Comparisons between a reference ON alpha cell (horizontal line) and two overlapping cells, an OFF alpha (solid bars) and an ON beta cell (stippled bars). H: Comparisons between a reference OFF alpha cell and two overlapping beta cells, one OFF (solid bars) and one ON (stippled bars). Cell locations (conventions as for Fig. 1): G: e = +4.4, s = –3.4; H: e = +4.7, s = –3.4. Scale bar = 20 μm.

those of the OFF alpha cell. They clearly costratified with the ON alpha's dendrites but extended substantially farther into the proximal part of sublamina b. Figure 4H displays a similar analysis for another triad of cells: an OFF alpha and a pair of beta cells (one ON and one OFF). The data were normalized to the depth of the OFF alpha dendrites (dashed line). Although the OFF alpha and OFF beta cells partially costratified, the OFF beta arbor extended substantially farther distally into sublamina a. There was no overlap in depth between the ON and the OFF beta dendrites, and a gap of several micrometers separated the ON beta arbor from that of the OFF alpha cell.

The discrepancies between the results obtained with the two methods are not surprising. In the through-focus analysis, the benchmarks for depth (i.e., the reference cell's processes at points of intersection) lay very close to the dendrite under study both in the plane of the retina and in depth. In the radial-section analysis, by contrast, the depth benchmarks (i.e., IPL boundaries) were more distant in depth and had to be located by horizontal interpolation when the nearest somatic profiles were laterally displaced from the point of measurement. For these reasons, the through-focus measurements were less influenced by undulations in the position or thickness of the IPL or its sublaminae. Taken together, the data suggest the laminar arrangement summarized in Figure 12. ON beta cells ramify broadly in sublamina b (S3 and S4), whereas OFF beta cells arborize throughout most of sublamina a. Alpha arbors ramify more narrowly than beta arbors: ON alphas costratify with the distal part of the ON beta arbor (in S3 and S3/4), whereas OFF alphas costratify with the proximal part of the OFF beta arbor (in S2 and S1/2). A small gap near the S2/3 border separates the ON and OFF arbors of both types.

Other ganglion cell types

We stained many ganglion cells that belonged to neither the alpha nor the beta morphological types. Generally, these cells had smaller somata and thinner axons than did alpha and beta cells. Dendritic structure varied widely among these cells, as reported by others (Wingate et al., 1992). In view of the widespread similarities between cat and ferret retina, including the presence of alpha and beta types, we reasoned that the ferret might possess homologues of several of the morphological types of ganglion cells described in cat retina. Here we provide evidence for at least six such types in ferret retina.

Most examples of each type possessed a well-filled axon in the optic fiber layer, but in some cases an axon could not be identified with certainty because of inadvertent bulk labeling of several axons in the vicinity of the cell or transection of the axon during somatic impalement. Such cells were left out of the following analysis unless they could be *unambiguously* identified as one of the following six types on the basis of their somadendritic structure and size at that retinal position. Assertions concerning the laminar positions of dendritic arbors are based partially on assessments of each cell's approximate depth of stratification relative to the borders of the IPL. These assessments were refined substantially by close examination of relative depth of dendritic stratification in 89 instances of overlap among two or more cells of different type (see Fig. 12B).

Delta cells (Fig. 6). We stained 25 ferret ganglion cells that closely resembled the delta or monoamine-accumulating ganglion cell type of the cat retina (Boycott and Wässle, 1974; Dacey, 1989). Ferret delta cells had small somata (mean diameter 15.4 μm; Table 1, Fig. 14) and large dendritic trees (mean diameter: 327 μm; Table 1, Fig. 13B). The dendritic profile was radiate in form, with only occasional recurving processes (Figs. 5A, 6). Dendrites branched with moderate frequency and at fairly regular intervals. Dendritic overlap was uncommon, though perhaps slightly more prevalent than is typical for cat delta cells. Terminal dendrites stratified narrowly in S1, largely or completely distal to the dendrites of OFF alpha cells (Fig. 12A,B). Cells with similar form but ramifying in sublamina b were not encountered in our material. Dendritic field size varied little over the retina (Fig. 13A).

Epsilon cells (Fig. 7). We encountered 26 cells that resembled the epsilon ganglion cell type of cat retina (Leventhal et al., 1980; Pu et al., 1994). These cells had small somata (mean diameter 16.3 μm; Table 1, Fig. 14) and radiating, sparsely branching dendritic trees (Figs. 5B, 7). Their dendritic fields were some of the largest we have observed among ferret ganglion cells (mean diameter 406 μm; Fig. 13B, Table 1) and exhibited no systematic topographic variation in size (Fig. 13A). Dendrites were generally smooth but in a few cells exhibited fine hair-like processes and spines. Dendrites were narrowly stratified in the middle of sublayer b of the IPL ($\sim$S4), where they costratified and lay partially proximal to those of ON alpha cells (Fig. 12A,B). We did not encounter cells with similar dendritic profiles ramifying in sublamina a.

Zeta cells (Fig. 8). Eighty-nine cells in our sample closely resembled zeta cells of the cat retina (Berson et al., 1998). These cells had among the smallest somata (mean diameter 13.7 μm; Table 1, Fig. 14), smallest dendritic arbors (mean diameter 160 μm; Table 1, Fig. 13B), and thinnest axons of all ferret ganglion cells. Terminal and preterminal dendrites were thin, densely branched, and studded with short twigs, spines, and hairs (Figs. 5C, 8). There was little overlap among dendrites, although some terminal branches closely approached one another or even made contact. Dendrites stratified narrowly at or near the a/b sublaminar border (S2/3) in the gap separating ON and OFF alpha dendrites (Fig. 12A,B). Dendritic fields were slightly smaller on average within the visual streak than in the superior or inferior periphery (Fig. 13A).

Eta cells (Fig. 9). Forty-two cells resembled the eta ganglion cell type of cat retina (Berson et al., 1999b). They had very small somata (mean diameter 14.0 μm; Table 1, Fig. 14) and thin axons. Their dendritic fields were small (mean diameter 195 μm; Table 1, Fig. 13B) and apparently varied little in size over the retina (Fig. 13A). Dendrites were thin and typically smooth, although in some cells they were moderately spiny. Dendrites generally followed courses that were roughly radiate in relation to the soma (Fig. 5D). However, their waviness, mutual overlap, and high branch frequency gave most profiles a tangled aspect. Branch density varied somewhat among cells; the cells illustrated in Figure 9A,B represent the extremes of the spectrum. Dendritic arbors stratified throughout most of sublamina a (Fig. 12A,B). Most of the processes costratified with those of overlapping OFF alpha cells, but some lay more distal in S1 (Fig. 12). No paramorphic type of sublamina b was encountered.

Theta cells (Fig. 10). We encountered 94 ferret ganglion cells resembling the theta cell, a bistratified cell type of the cat retina (Isayama et al., 2000). Ferret theta cells had very small somata (mean diameter 13.7 μm; Table 1, Fig. 14) and small

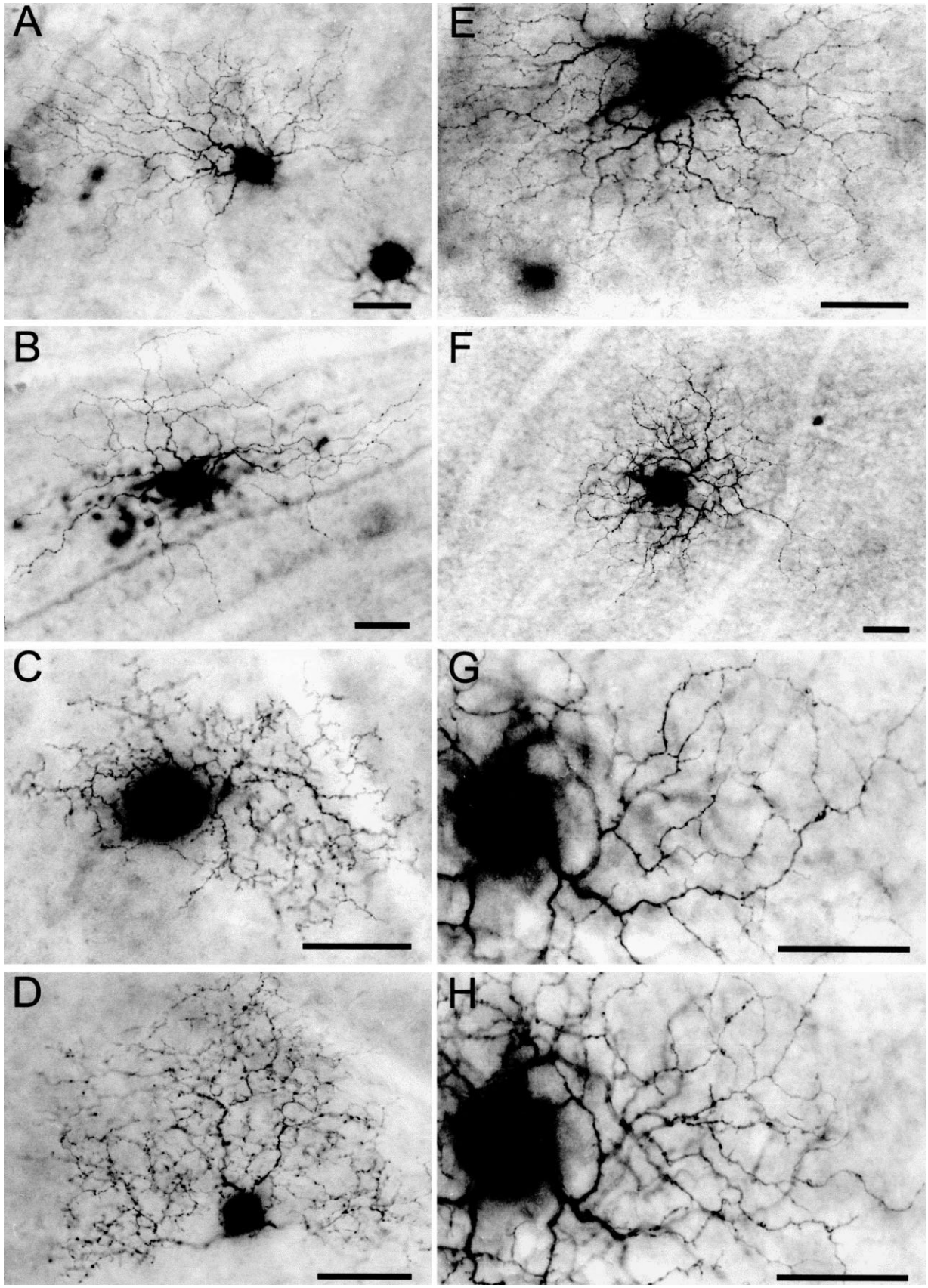

Figure 5.
Photomicrographs of representative ferret non-alpha/non-beta ganglion cells. **A:** Low-power micrograph of a delta cell. Cell location (conventions as for Fig. 1): e = +0.6 mm, s = +0.6 mm. **B:** Low-power micrograph of a epsilon cell: e = +4.2 mm, s = –1.7 mm. **C:** Low-power micrograph of a zeta cell: e = +5.2 mm, s = +1.5 mm. **D:** Low-power micrograph of an eta cell: e = +3.0 mm, s = +2.7 mm. **E:** Low-power micrograph of a theta cell: e = +5.1 mm, s = –4.6 mm. **F–H:** An iota cell, shown at low magnification (F) and at higher magnification at planes of focus corresponding to the proximal (G) and distal (H) dendritic arbors. Cell location: e = 5.8 mm, s = –0.6 mm. Scale bars = 50 μm.

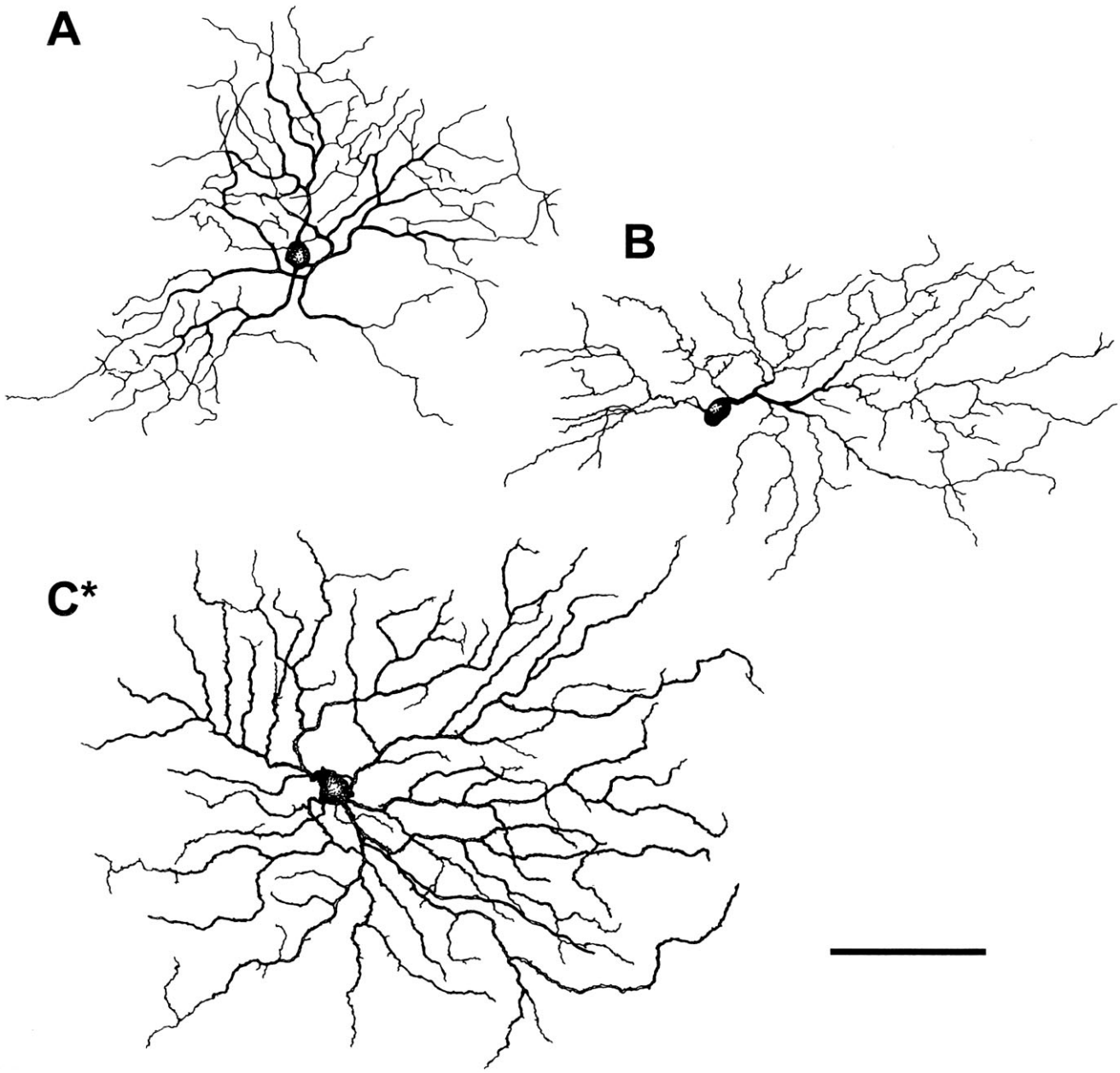

Figure 6.
Camera lucida drawings of representative delta ganglion cells of the ferret (**A,B**) and cat (**C**) retina. Asterisk in this and subsequent figures indicates examples from the cat. Axons omitted for clarity. Cell locations (conventions as for Fig. 1): A: e = +5.4 mm, s = +5.2 mm; B: e = −0.9 mm, s = −0.6 mm; C: e = +3.5 mm, s = +1.8 mm. Scale bar = 100 μm.

dendritic arbors (mean diameter 183 μm; Fig. 13B, Table 1). Dendritic profiles were very complex, displaying denser branching and more extensive overlap than any other ferret ganglion cell type (Fig. 10). Dendrites meandered chaotically, bearing no consistent orientation relative to the soma. The dendrites were thin and appeared moderately varicose in most cases (Fig. 5E) and some had a number of spines. Dendrites were concentrated in two strata lying on either side of the a/b sublaminar border and corresponded to the levels of stratification of the ON and OFF alpha cells (Fig. 12A,B). This bistratification was obscured somewhat by the large number of dendritic segments bridging the two strata but was detectable throughout the arbor except for a few areas of sparser branching. Overall, the density of branching was comparable in the two strata, but in a few cells total dendritic length appeared greater in either the proximal or the distal tier. Dendritic fields were slightly smaller on average in the visual streak than elsewhere (Fig. 13A).

Iota cells (Fig. 11). We stained 30 ganglion cells strikingly similar to the iota cell of cat retina, a bistratified type pre-

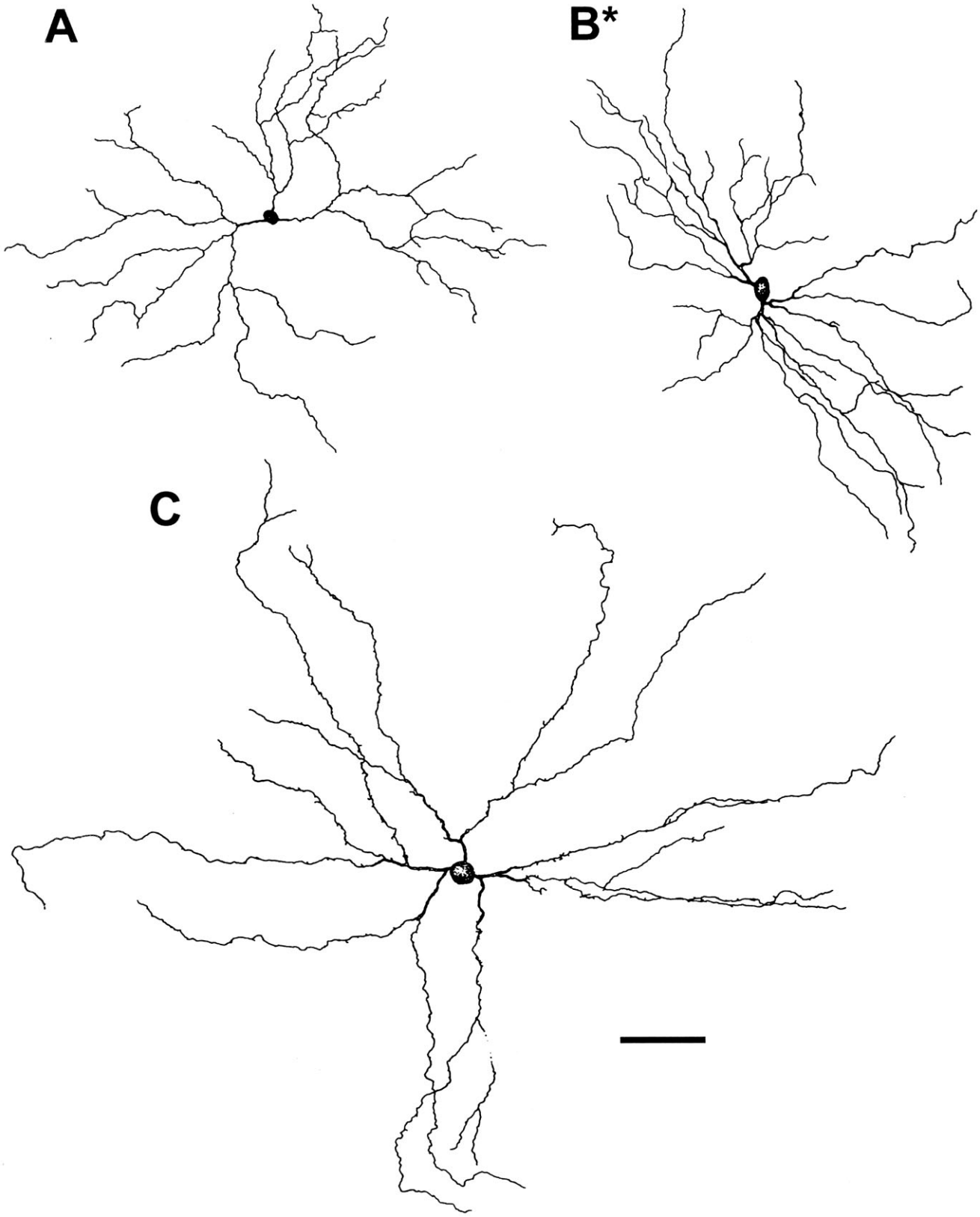

Figure 7.
Camera lucida drawings of epsilon ganglion cells of the ferret (**A,C**) and cat (**B**) retina. Axons omitted for clarity. Cell locations (conventions as for Fig. 1). A: e = +4.9 mm, s = +1.8 mm; B: e = +2.4 mm; C: e = +2.2 mm; s = +2.2 mm. Scale bar = 100 μm.

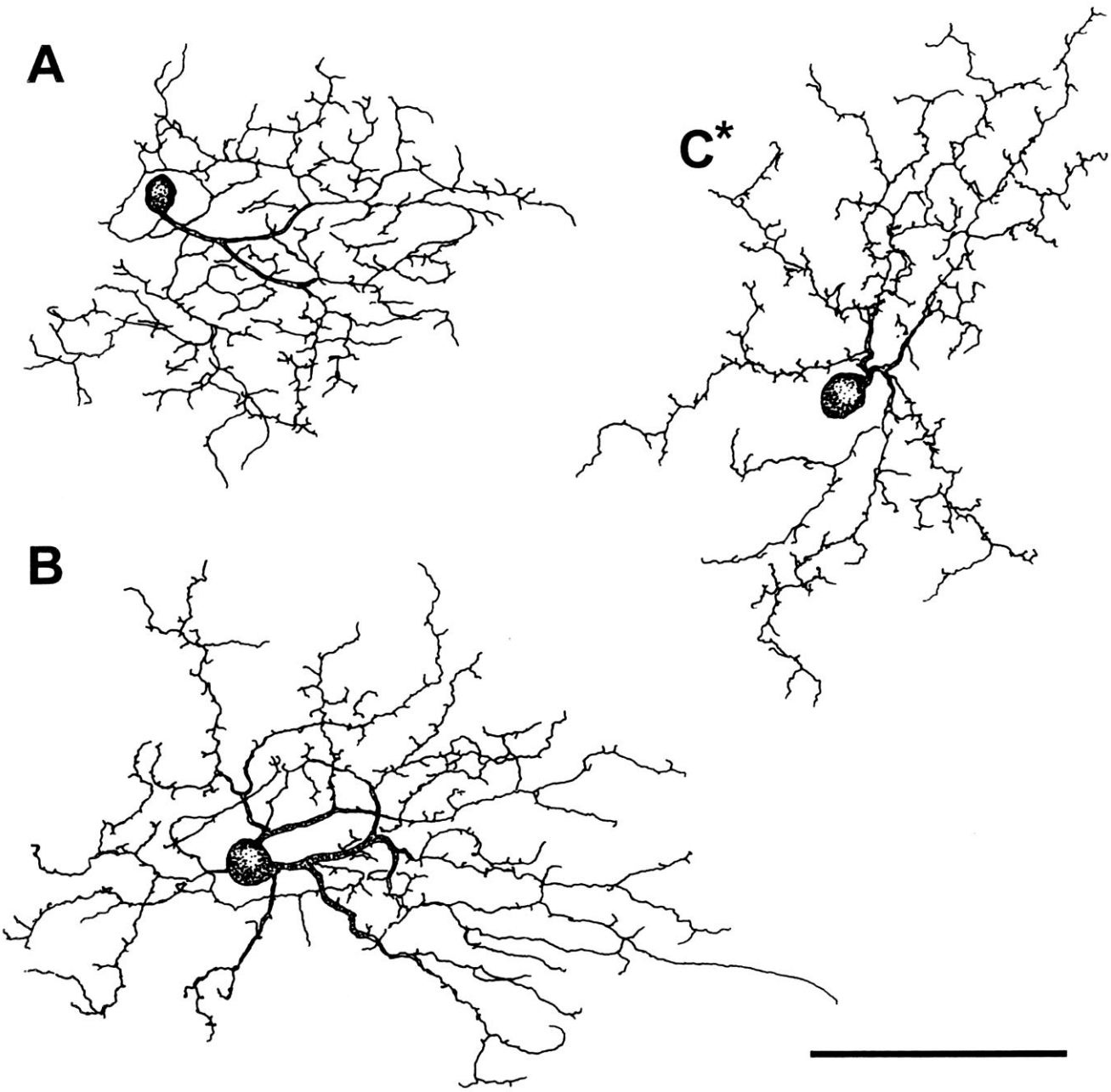

Figure 8.
Camera lucida drawings of zeta ganglion cells of the ferret (**A,B**) and cat (**C**) retina. Axons omitted for clarity. Cell locations (conventions as for Fig. 1): A: e = +4.1 mm; s = +1.0 mm; B: e = +6.1 mm, s = +0.3 mm; C: e = +6.4 mm; s = −0.2 mm. Scale bar = 100 μm.

sumed to correspond to the ON-OFF direction-selective cell (Famiglietti, 1987; Berson et al., 1997; O'Brien et al., 1999, 2002). In ferrets, as in cats, iota cells shared many similarities with theta cells. Viewed en face, they exhibited richly branched profiles with extensive dendritic overlap (Figs. 5F–H, 11A,B). Their bistratified dendrites ramified in roughly the same two strata as those of theta cells (Fig. 12A,B) but had many fewer dendrites interconnecting the two strata. This made it much easier to discern the inner and outer arbors, which individually exhibited little or no dendritic overlap (Figs. 5G,H, 11B). In addition, iota cells had larger dendritic fields (mean diameter 304 μm; Table 1, Fig. 13B), thicker dendrites, lower branching density, and larger somata (mean diameter 15.4 μm; Table 1, Fig. 14) than theta cells. Dendritic fields tended to be slightly smaller in the visual streak than elsewhere (Fig. 13A).

Unidentified varieties. The great majority of the cells in our sample belonged to one of the types described above. The remaining cells were most likely encountered in cat retina as well, but these morphological types were not studied ex-

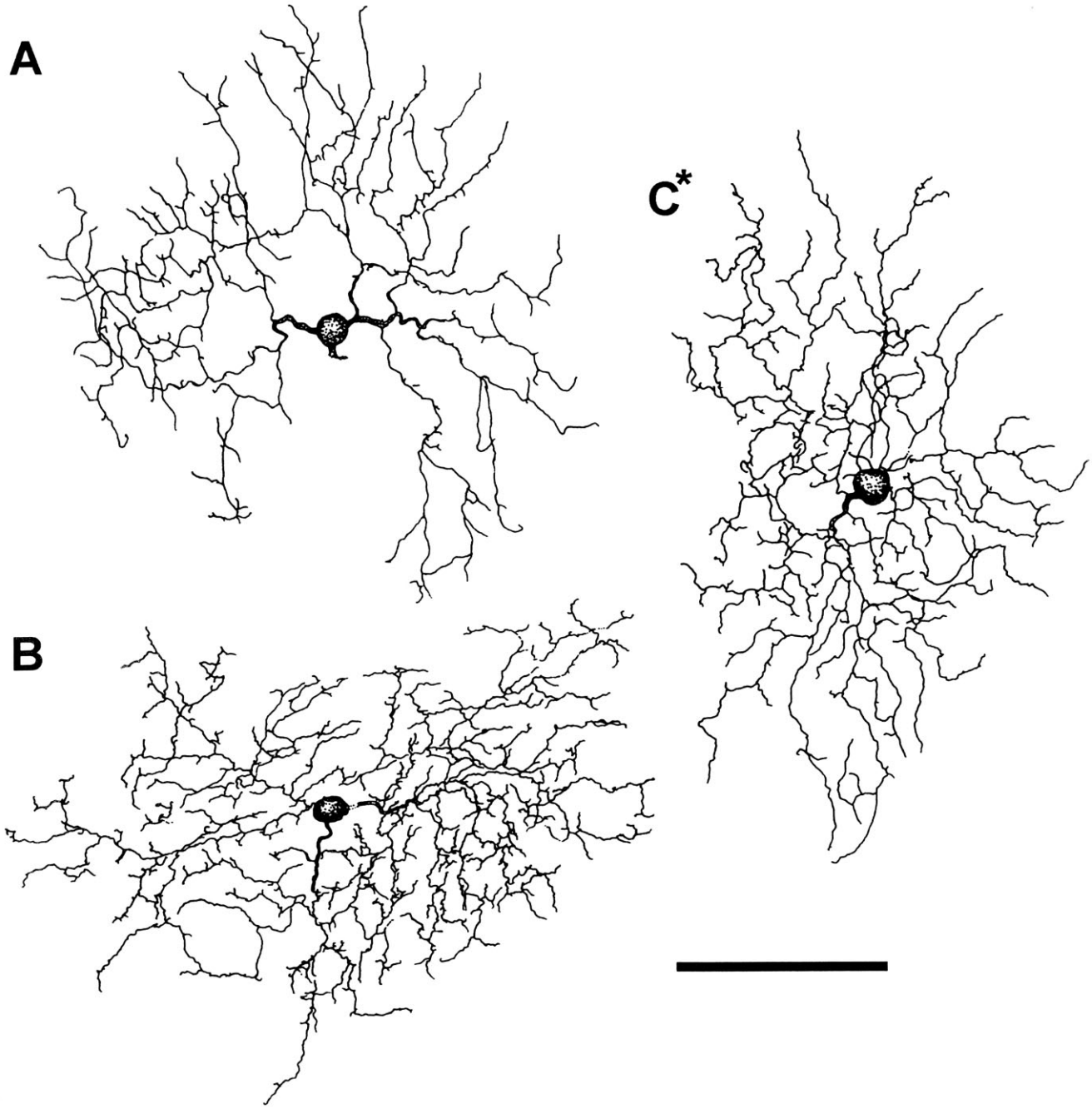

Figure 9.
Camera lucida drawings of eta ganglion cells of the ferret (**A,B**) and cat (**C**) retina. Axons omitted for clarity. Cell locations (conventions as for Fig. 1): A: e = +4.8 mm, s = +1.8 mm; B: e = +3.9 mm; s = +2.9 mm; C: e = +6.0 mm; s = +0.6 mm. Scale bar = 100 μm.

tensively in either species, so rigorous comparisons were not made. These unclassified ganglion cells all had dendritic fields at least as large as those of delta and iota cells and branching densities lower than those of zeta and theta cells. Otherwise these cells were heterogeneous in form. Some were narrowly stratified; others were bistratified or ramified diffusely in both a and b sublaminae. We also stained large numbers of presumed displaced amacrine cells in the GCL. These cells lacked axons in the optic fiber layer, although some extended multiple axon-like processes into the IPL. Cell bodies were typically smaller than those of ganglion cells, but there was substantial overlap between the populations. Several of the amacrine cells clearly resembled those reported among cat amacrine cells, but we have not studied them in detail.

Quantitative comparisons among types. Here we summarize some of the quantitative criteria by which the 10 gan-

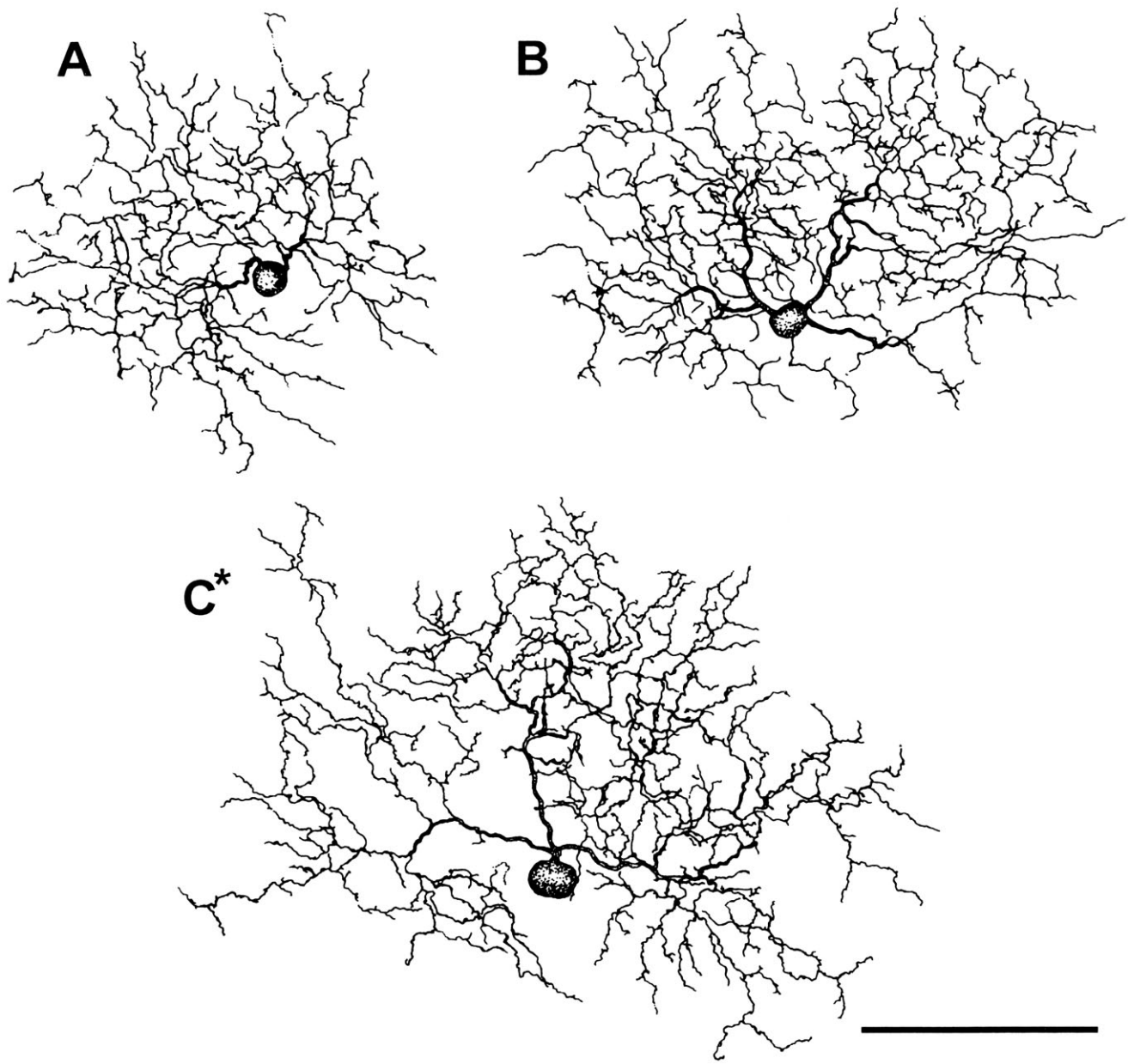

Figure 10.
Camera lucida drawings of theta ganglion cells of ferret (**A,B**) and cat (**C**) retina. Axons omitted for clarity. Cell locations (conventions as for Fig. 1): A: e = +1.3 mm, s = +1.3 mm; B: e = +3.5 mm, s = +3.3 mm; C: e = +1.5 mm, s = +1.3 mm. Scale bar = 100 μm.

glion cell types studied here may be distinguished. Figure 12 summarizes patterns of dendritic stratification. Four types ramify exclusively in sublamina a. Among these, the OFF alpha and delta cells are both relatively narrowly stratified but ramify in largely distinct strata of the OFF sublamina. The others, the OFF beta and eta cells, ramify broadly throughout the OFF sublayer. Three types ramify exclusively in sublamina b, the ON alpha rather narrowly and the ON beta and epsilon cells more broadly. One type, the zeta cell, ramifies narrowly at the a/b sublaminar border and exhibits minimal overlap in depth with ON alpha, ON beta, or OFF alpha cells. The remaining two types (theta and iota) are bistratified; for both types, the distal arbor costratifies with dendrites of OFF alpha cells and the proximal arbor with those of ON alpha cells.

Figure 13 and Table 1 compare the dendritic field sizes of ferret ganglion cell types that fall within four broad ranges. Beta cells have the smallest dendritic fields at all retinal locations. The next smallest are the zeta, eta, and theta cells, with substantial overlap among these types. Iota and delta cells have medium-sized dendritic profiles, whereas alpha and epsilon cells have the largest fields of all types studied.

Figure 14 and Table 1 compare soma diameters among these types. Alpha cells had the largest cell bodies, whereas

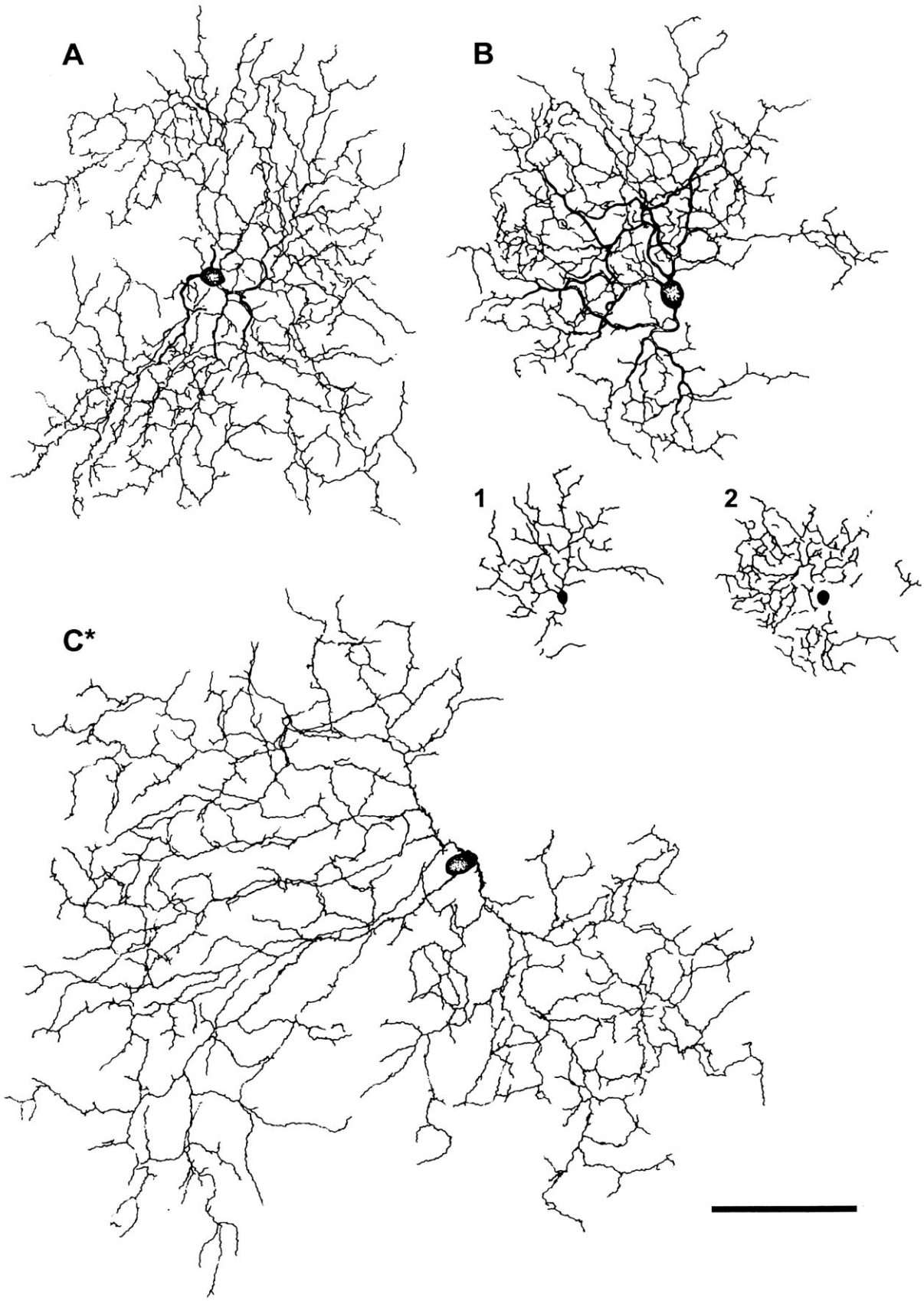

Figure 11.
Camera lucida drawings of iota ganglion cells of the ferret (**A,B**) and cat (**C**). Inner (1) and outer (2) arbors are displayed separately at reduced magnification for the cell in B. Axons omitted for clarity. Cell locations (conventions as for Fig. 1): A: e = +6.1 mm, s = +0.2 mm; B: e = +3.5 mm, s = +3.2 mm; C: e = +4.0 mm, s = +3.8 mm. Scale bar = 100 μm.

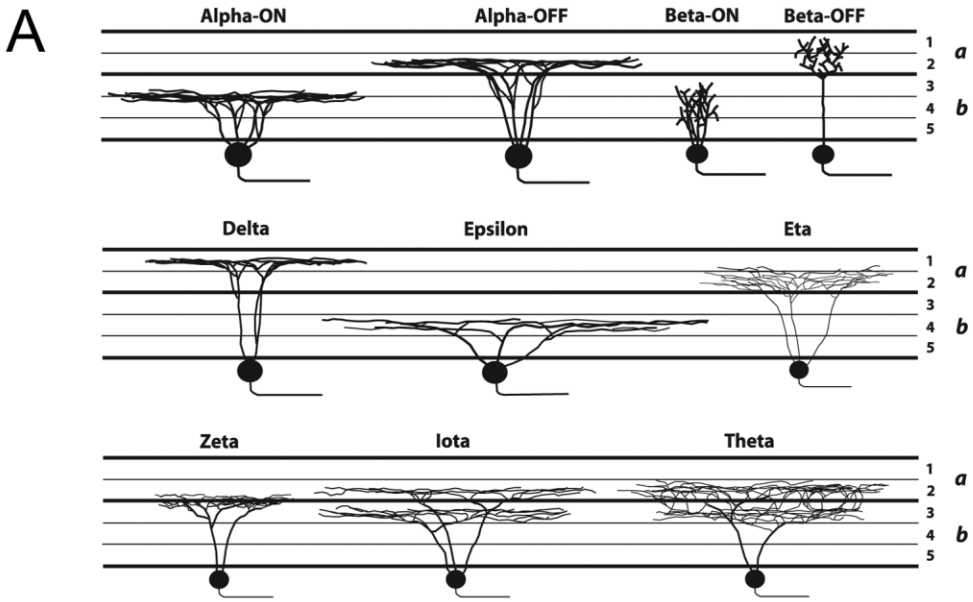

B

	Alpha OFF	Beta ON	Beta OFF	Delta	Epsi-lon	Zeta	Eta	Theta ON	Theta OFF	Iota ON	Iota OFF
Alpha ON	⇩ 25	↔↑ 7	⇩ 5	⇩ 1	↑↔ 8	⇩ 8	⇩ 2	↔ 8	⇩ 8	↔ 1	⇩ 1
Alpha OFF		↑ 12	↔⇩ 10	⇩ 5	↑ 3	↑ 9	↔⇩ 3	↑ 9	↔ 9	↑ 3	↔ 3
Beta ON			⇩ 7	⇩ 3	↑↔ 5	⇩ 2					
Beta OFF				⇩↔ 3	↑ 2			↑ 1	↔↑ 1		
Delta					↑ 2	↑ 1		↑ 1	↑ 1	↑ 1	↑ 1
Epsi-lon						⇩ 1		⇩↔ 2	⇩ 2		
Zeta								↑ 2	⇩ 2	↑ 1	⇩ 1
Eta								↑ 1	↔ 1		
Theta ON									⇩ 94	↔ 1	⇩ 1
Theta OFF										↑ 1	↔ 1
Iota ON											⇩ 30

Figure 12.
Comparisons of dendritic stratification among ganglion cell types of the ferret retina. **A:** Schematic radial section of the inner plexiform layer (IPL) summarizing the patterns of dendritic stratification inferred for each type from the data in Figure 4 and other through-focus observations as described in text. S1–S5: strata 1–5 of the IPL. Dashed line marks the boundary between the OFF sublamina (a) and the ON sublamina (b). **B:** Summary of data on relative depth of stratification of various types obtained by through-focus inspection of overlapping dendritic arbors. Symbols in each cell of the matrix indicate whether the ganglion cell type listed to the left (row heading) stratifies proximally (downward arrows), at the same depth (double-headed arrows), or distally (upward arrows) to the type listed above (column heading). Numbers indicate the number of overlapping arbors studied. For the bistratified types (theta and iota), the inner (ON) and outer (OFF) arbors are considered separately.

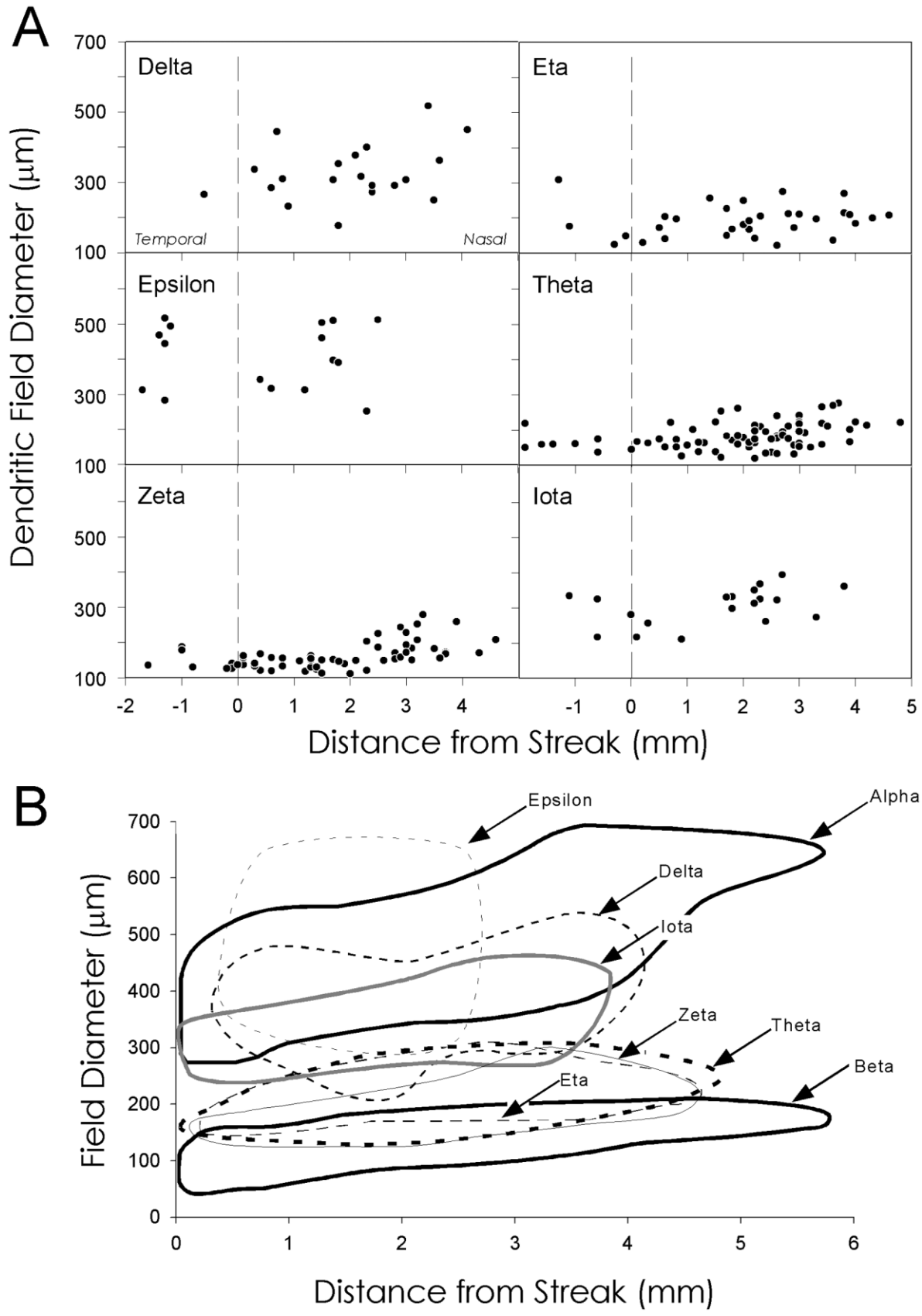

Figure 13.
Comparison of dendritic field size among six non-alpha, non-beta ganglion cell types of the ferret retina. **A:** Dendritic field diameters of each type as a function of distance from the axis of the visual streak. Negative eccentricities correspond to locations in the temporal hemiretina. Statistics for each type are given in Table 1. **B:** Comparison among these types and with alpha and beta cells of the ferret retina. Each outline represents the envelope of the field size distribution of a single type, drawn from data shown in Figures 3B and 13A. No distinction has been made between nasal and temporal hemiretinas.

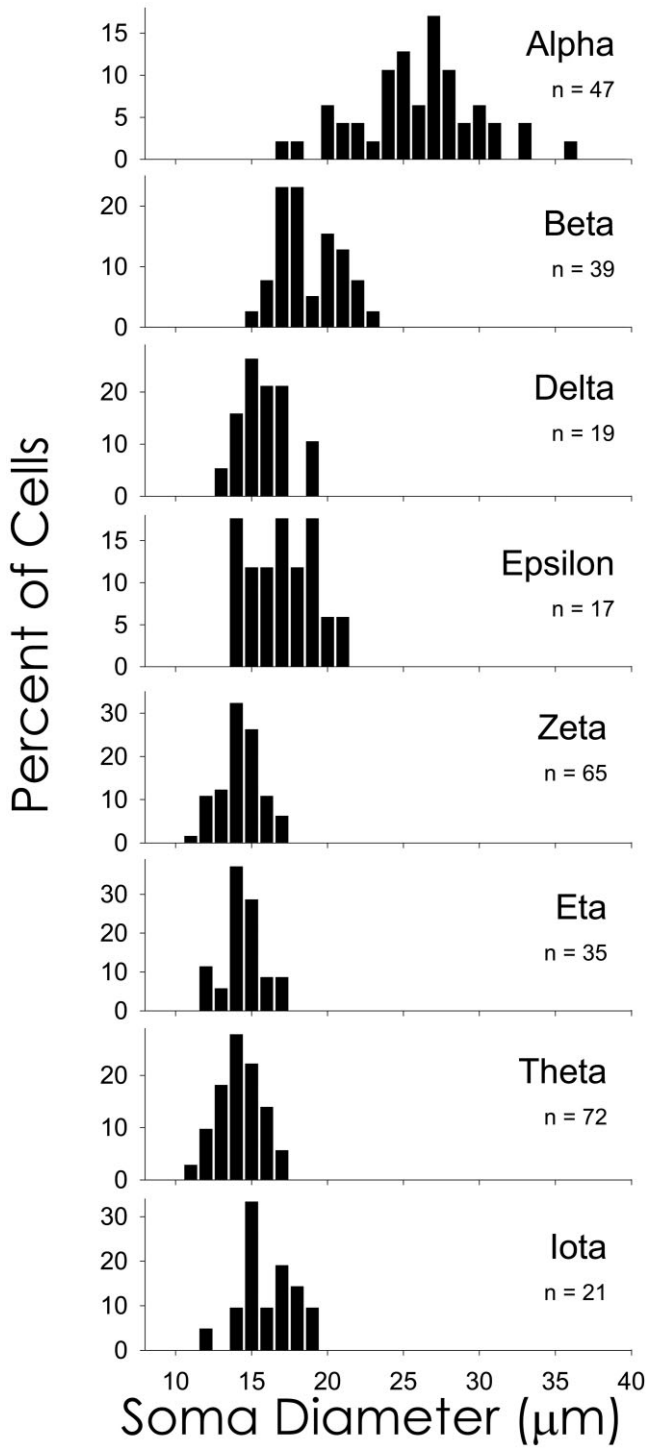

Figure 14.
Comparison of soma size among ferret ganglion cell types. Statistics for each type are given in Table 1.

beta cells were intermediate in size. The remaining types form two groups: delta, epsilon, and iota cells have small to medium-sized cell bodies, and the zeta, eta, and theta cells have very small somata. Nonetheless, there is substantial overlap among the soma size distributions of virtually all types.

DISCUSSION

The present study extends earlier descriptions of the morphology of alpha and beta ganglion cells of the ferret retina with respect to the dendritic stratification and topographic variations in dendritic field dimensions. In addition, it provides evidence for the presence of at least six additional ganglion cell types in ferret retina, each with a clear counterpart in cat retina.

Morphology of ferret alpha and beta cells

Our data confirm and extend prior work demonstrating the existence of alpha and beta cells in ferret retinas (Vitek et al., 1985; Amthor and Jackson, 1986; Peichl et al., 1987b; Wingate et al., 1992; Penn et al., 1994). The dendritic profiles of ferret alpha and beta cells are very similar to their counterparts in cat retina (Boycott and Wässle, 1974; Kolb et al., 1981; Wässle and Boycott, 1991; Stein et al., 1996). Both types occur as paramorphic pairs (i.e., as forms virtually identical in morphology except for their stratification in different layers of the IPL; see, e.g., Famiglietti and Kolb, 1976). In both species, alpha cell dendritic fields are about three to five times larger in diameter than beta cell fields at any retinal eccentricity, with no overlap between the two types (Boycott and Wässle, 1974; Kolb et al., 1981; Vitek et al., 1985; Wingate et al., 1992).

Alpha cells are apparently a universal feature of the mammalian retina, with a strongly conserved pattern of dendritic stratification (Peichl et al., 1987b). Our quantitative assessment shows that ferret alpha cells conform to this stratification pattern, as anticipated by the qualitative observations of Peichl et al. (1987b). Compared with ferret beta cells, alpha cells have more narrowly stratified arbors. Our data also confirm the existence of ON and OFF subtypes of beta cells in ferret retina (Kageyama and Wong-Riley, 1984; Wingate et al., 1992) and show that their stratification pattern is comparable to that reported for beta cells of the cat retina (Famiglietti and Kolb, 1976; Watanabe et al., 1985; McGuire et al., 1986; Weber et al., 1991).

Topography of alpha and beta cells

Individual ganglion cell types form mosaics that preserve a characteristic amount of dendritic overlap among members despite large topographic variations in scale (Wässle and Boycott, 1991). One virtue of these mosaics is that they ensure that each type covers or "tiles" the retinal surface, without gaps. They also ensure that every point in the retinal image falls within the receptive field centers of about the same number of cells of each type, regardless of location. In addition, they may ensure a match between the spatial resolution of individual type members and the Nyquist limit set by the spacing of type members, an arrangement that optimizes spatial acuity while avoiding aliasing (for review see Wässle and Boycott, 1991).

The ferret is in many ways an ideal species in which to study the ontogenetic mechanisms that form such mosaics. Many of these processes occur postnatally in ferret ganglion cells, including outgrowth, differentiation of branching patterns, activity-dependent segregation of dendritic arbors within specific laminae of the IPL, and programmed cell death leading to

regional variations in ganglion cell density (see the introductory paragraphs). There is, however, little direct evidence that ferret ganglion cells form regular dendritic mosaics. Indeed, it has been questioned whether alpha or beta cells exhibit an inverse relationship between dendritic field size and local density, a prerequisite for such mosaics. Although such a relationship received some initial support from retrograde filling studies (Vitek et al., 1985) and was corroborated for alpha cells by reduced silver methods (Peichl et al., 1987b), it was subsequently called into question for both alpha and beta cells on the basis of intracellular staining (Wingate et al., 1992).

Our own data support a systematic relationship between alpha and beta cell field size and retinal topography. Moreover, the magnitude of the systematic variation in field area is comparable to that of the topographic variation in density, as required by a mosaic with uniform dendritic overlap (Wässle and Boycott, 1991). The density of all ganglion cells and of alpha cells varies four- to eightfold over the region studied (Henderson, 1985; Vitek et al., 1985; Peichl et al., 1987b). This predicts that mean dendritic field diameter of each type should vary about 2- to 2.8-fold, close to the observed values of 1.7-fold for alpha cells and 2.7-fold for beta cells (Fig. 3B, Table 2). The fact that beta cells exhibit a larger proportional variation in field size than do alpha cells implies that beta cells have a steeper topographic gradient in cell density. In other words, beta cells make up a larger fraction of the ganglion cell population in the central retina than in the periphery. This appears to be true also for beta cells of cat retina (Stein et al., 1996) and midget cells in the primate retina, which may be a homologous cell type (Rodieck et al., 1985; Dacey and Brace, 1992).

The negative result of Wingate et al. (1992) concerning such topographic dependence is attributable to the indirect method used for estimating ganglion cell density together with weak systematic variation in field size. Topographic gradients in beta and alpha cell field size (and, by inference, cell density) are far more modest in ferret than in cat retina. Among alpha cells, mean local field diameter varies less than twofold in ferrets compared with fourfold in cats. For beta cells, the variation is only threefold in ferrets compared with tenfold in cats (Boycott and Wässle, 1974; Kolb et al., 1981; Stein et al., 1996; Berson et al., 1998).

Generally, alpha and beta cell dendritic fields are about the same size in the two species. In the central retina, however, they are substantially larger in ferret than in cat. Because beta-cell resolution seems likely to be a limiting factor in spatial acuity among the Carnivora (see Stein et al., 1996), this difference in itself suggests lower maximum acuity in ferrets than in cats. This difference is amplified by the ferret's smaller eye and lower retinal magnification (i.e., millimeters of retina per degree of visual angle) and accounts in part for the lower spatial resolution of ferret geniculate neurons compared with those in cat (Price and Morgan, 1987). A further point of distinction between ferret and cat retina is in the relative development of the area centralis and visual streak. In the ferret, the streak is more prominent than that in the cat, whereas the area centralis is less so. This is evident in maps of ganglion cell density and in plots of field size as a function of retinal location (see, e.g., Boycott and Wässle, 1974; Wässle et al., 1975; Hughes, 1981; Henderson, 1985; Vitek et al., 1985; Peichl et al., 1987b; Wong and Hughes, 1987; Stein et al., 1996). The visual streak is a prominent retinal feature in vertebrates inhabiting open terrain and may facilitate a form of panoramic vision; the area or fovea centralis is best developed in vertebrates with high acuity binocular vision and well-developed gaze control (Hughes, 1977; Stone, 1983). Differences between ferrets and cats in retinal topography may thus reflect distinctions in visual ecology.

Other ganglion cells

Substantial morphological heterogeneity has been observed among ferret ganglion cells that are neither alpha nor beta cells (Vitek et al., 1985; Wingate et al., 1992). By analogy with work in other vertebrate retinas, it seems reasonable to assume that these cells comprise a large set of morphologically distinct types, each with a characteristic pattern of dendritic branching, field size, stratification, retinal topography, and central projection (Rodieck and Brening, 1983; Stone, 1983; Wässle and Boycott, 1991). Wingate et al. (1992) took an initial step toward developing a classification scheme for these ganglion cells by dividing their sample of intracellularly stained ganglion cells into three broad groups (termed *tight*, *loose*, and *sparse*) that differed in dendritic complexity and patterns of central projection. However, there is substantial intragroup heterogeneity with respect to branching structure and stratification. To provide a basis for understanding this diversity, we explored the possibility that the ferret's ganglion cell population contains counterparts of many of the ganglion cell types that have been identified in cat retina. This approach was anticipated by Vitek et al. (1985), who identified a likely equivalent of the cat's epsilon cell among ferret retinal ganglion cells stained by retrograde transport. Here, we confirm and extend that observation and provide evidence that the ferret retina possesses counterparts of at least five additional cat ganglion cell types: delta, zeta, eta, theta, and iota. The present findings suggest that each of these morphological classes represents a "natural type," empirically demonstrable by the covariation of its members on many independent morphometric dimensions and by the absence of intermediate forms (Rowe and Stone, 1977; Rodieck and Brening, 1983).

This provisional taxonomy is by no means exhaustive. Although we believe that the great majority of ferret ganglion cells belong to one of the types identified here, both our sample and that of Wingate et al. (1992) contain cells that apparently do not. Similarities between such cells in the ferret and those qualitatively surveyed in the cat retina (see, e.g., Kolb et al., 1981) suggest that further parallels in ganglion cell typology in these species will emerge.

The dendritic fields of each type are generally of about the same absolute size in the two species but, because of differences in retinal magnification, are substantially larger in ferret than in cat when expressed in terms of visual angle. The rank order of these types by field size is very similar in the two species, suggesting that their relative frequency may be similar.

Delta cells. We identified delta cells in the ferret retina (Fig. 6) similar to those in cats (Boycott and Wässle, 1974; Wässle et al., 1987; Dacey, 1989; see also G18 and G19 of Kolb et al., 1981). Wingate and colleagues (1992) included presumptive delta cells within their loose group (see especially cell vii of their Fig. 9 and the loose cells of Fig. 19).

According to Wingate et al. (1992), loose cells project ipsilaterally from the temporal retina and innervate both the midbrain and the thalamus, properties they share with cat delta cells (D.M. Berson and M. Pu, unpublished observations). In cat retina, delta cells accumulate exogenous monoamines and correspond to OFF center tonic W-cells (Wässle et al., 1987; Dacey, 1989; O'Brien et al., 1999). In agreement with the description of cat delta cells by Dacey (1989) and Kolb et al. (1981), we did not encounter a paramorphic counterpart of the delta cell stratifying in the ON sublamina in ferrets. These data contrast with those of Wässle et al. (1987) and Peichl (1989), who described delta cells with dendrites stratifying in sublamina b in cats and rats, respectively.

Epsilon cells. Epsilon cells in the ferret (Fig. 7) closely resembled those in the cat (Leventhal et al., 1980; Pu et al., 1994). In cat, they correspond to ON center tonic W-cells and perhaps also to Q cells (Pu et al., 1994; Troy et al., 1995). A similar morphological type has been described in the retinas of primates (Leventhal et al., 1981; Rodieck and Watanabe, 1993) and dogs (Fig. 4k of Peichl, 1992). Epsilon cells appear to represent the predominant type within the sparse group of ferret ganglion cells (Wingate et al., 1992; see especially cell x of their Fig. 9 and the sparse cells of Fig. 19, top). However, other types were apparently included among the sparse cells by Wingate and colleagues, because some of them, unlike epsilon cells, ramified in sublamina a. Sparse cells in the ferret apparently innervate both the midbrain and the thalamus and project ipsilaterally from the temporal retina (Wingate et al., 1992), properties they share with cat epsilon cells (Pu et al., 1994).

Zeta cells. Zeta cells in ferrets (Fig. 8) and in cats (Berson et al., 1998) had among the smallest fields, and the tiniest of these present in the visual streak, suggesting a strong tendency to concentrate there (Fig. 13; Berson et al., 1998). In cat, zeta cells correspond to an ON-OFF phasic W cell, also known as a local edge detector (Berson et al., 1998; O'Brien et al., 1999). Zeta cells bear a strong resemblance to the local edge detectors in rabbit retina (Amthor et al., 1989; van Wyk et al., 2006) and may be homologous to the maze cell of macaque retina (Rodieck and Watanabe, 1993). Zeta cells were encountered in the ferret retina by Wingate et al. (1992; see cells i, iv and the cell just below iv in their Fig. 9 and also their Fig. 10C). They included these cells within the group they termed *tight*, which we believe also includes eta cells and possibly also theta cells (see below). According to Wingate et al. (1992), tight cells project contralaterally from the temporal retina, a property they share with cat zeta cells (Berson et al., 1998).

Eta cells. Eta cells in both ferrets (Fig. 9) and cats (Berson et al., 1999b) have moderately small, densely branched arbors that stratify broadly in sublamina a. Ferret eta cells were encountered by Wingate et al. (1992) and included by them in their tight group (see their Fig. 9, cells ii and v). For cat retina, it has been suggested they correspond to phasic OFF center W cells (Berson et al., 1999b; O'Brien et al., 1999). Cat eta cells project ipsilaterally from the temporal retina, whereas ferret tight cells project contralaterally (Wingate et al., 1992; Berson et al., 1999b).

Theta cells. Theta cells are found in both cats (Isayama et al., 2000) and ferrets (Fig. 10) but might not have been encountered in earlier studies of ferret retina, insofar as bistratified ganglion cell types were not reported previously. Bistratification in theta cells can easily be overlooked because of the extensive cross-linking of the ON and OFF arbors. At least one tight cell illustrated by Wingate et al. (1992; Fig. 9, cell iii) closely resembles a theta cell. In cats, theta cells project to the lateral geniculate complex as well as the superior colliculus (Isayama et al., 2000). Preliminary evidence suggests that cat theta cells are ON-OFF phasic W cells (O'Brien et al., 1999).

Iota cells. Iota cells in ferrets (Fig. 11), like those in cats (Berson et al., 1997), have bistratified dendritic arbors of intermediate size. Wingate et al. (1992) did not encounter this type, insofar as they observed no bistratified forms. Both ferret and cat iota cells closely resemble the type I bistratified cell of rabbit, the morphological counterpart of the ON-OFF direction-selective cell (Amthor et al., 1984, 1989; Famiglietti, 1992; Yang and Masland, 1992; Oyster et al., 1993; Vaney, 1994; Yang and Masland, 1994; O'Brien et al., 1999).

CONCLUSIONS

The present study advances our understanding of the ganglion cell types present in the ferret retina, including their topographic organization and patterns of stratification. The findings demonstrate a remarkable degree of similarity to ganglion cell organization in the cat, despite lower retinal magnification and shallower topographic gradients in cell density and field size. Most of the same morphological types that have been described so far in the cat retina are represented in the ferret. Their relative field dimensions and stratification patterns are virtually indistinguishable from their counterparts in cat retina. Alpha cells, beta cells, and at least some other types exhibit an inverse relationship between dendritic field dimensions and ganglion cell density, as expected for regular ganglion cell mosaics. Taken together with the altricial development of the ferret visual system, the results underscore the promise of the ferret retina as a model system for studies of the differentiation of individual ganglion cell types, including their specific patterns of dendritic stratification and the generation of characteristic sampling arrays.

ACKNOWLEDGMENTS

We thank Dr. Michael Baum for his gift of several ferrets, Dr. Dennis Dacey for guidance on preparation of radial sections, and Vikas Tewari for assistance with the morphometric analysis.

LITERATURE CITED

Amthor FR, Jackson CA. 1986. Staining of retinal neurons in the isolated eyecup by extracellular horseradish peroxidase injection. Vis Res 26: 269–274.

Amthor FR, Oyster CW, Takahashi ES. 1984. Morphology of on-off direction-selective ganglion cells in the rabbit retina. Brain Res 298: 187–190.

Amthor FR, Takahashi ES, Oyster CW. 1989. Morphologies of rabbit retinal ganglion cells with complex receptive fields. J Comp Neurol 280:97–121.

Berson DM, Isayama T, Pu M. 1997. Morphology of presumed ON-OFF direction selective ganglion cell of cat retina. Soc Neurosci Abstr 23:730.

Berson DM, Pu M, Famiglietti EV. 1998. The zeta cell: a new ganglion cell type in cat retina. J Comp Neurol 399:269–288.

Berson DM, Isayama T, O'Brien BJ, Pu M. 1999a. The kappa ganglion cell type of cat and ferret retina. Invest Ophthalmol Visual Sci 40:S813.

Berson DM, Isayama T, Pu M. 1999b. The eta ganglion cell type of cat retina. J Comp Neurol 408:204–219.

Bodnarenko SR, Jeyarasasingam G, Chalupa LM. 1995. Development and regulation of dendritic stratification in retinal ganglion cells by glutamate-mediated afferent activity. J Neurosci 15:7037–7045.

Bodnarenko SR, Yeung G, Thomas L, McCarthy M. 1999. The development of retinal ganglion cell dendritic stratification in ferrets. Neuroreport 10:2955–2959.

Boycott BB, Wässle H. 1974. The morphological types of ganglion cells of the domestic cat's retina. J Physiol 240:397–419.

Coombs J, van der List D, Wang GY, Chalupa LM. 2006. Morphological properties of mouse retinal ganglion cells. Neuroscience 140:123–136.

Dacey DM. 1989. Monoamine-accumulating ganglion cell type of the cat's retina. J Comp Neurol 288:59–80.

Dacey DM, Brace S. 1992. A coupled network for parasol but not midget ganglion cells in the primate retina. Vis Neurosci 9:279–290.

Famiglietti EV. 1987. Starburst amacrine cells in cat retina are associated with bistratified, presumed directionally selective, ganglion cells. Brain Res 413:404–408.

Famiglietti EV. 1992. Dendritic co-stratification of ON and ON-OFF directionally selective ganglion cells with starburst amacrine cells in rabbit retina. J Comp Neurol 324:322–335.

Famiglietti EV Jr, Kolb H. 1976. Structural basis for ON- and OFF-center responses in retinal ganglion cells. Science 194:193–195.

Greiner JV, Weidman TA. 1981. Histogenesis of the ferret retina. Exp Eye Res 33:315–332.

Henderson Z. 1985. Distribution of ganglion cells in the retina of adult pigmented ferret. Brain Res 358:221–228.

Henderson Z, Finlay BL, Wikler KC. 1988. Development of ganglion cell topography in ferret retina. J Neurosci 8:1194–1205.

Hughes A, editor. 1977. Topography of vision in mammals of contrasting life style: comparative optics and retinal organisation, 5th ed. Berlin: Springer-Verlag. p 613–756.

Hughes A. 1981. Population magnitudes and distribution of the major modal classes of cat retinal ganglion cell as estimated from HRP filling and a systematic survey of the soma diameter spectra for classical neurones. J Comp Neurol 197:303–339.

Isayama T, Berson DM, O'Brien BJ, Pu M. 1999. The lambda ganglion cell type of cat and ferret retina. Invest Ophthalmol Vis Sci 40:S813.

Isayama T, Berson DM, Pu M. 2000. Theta ganglion cell type of cat retina. J Comp Neurol 417:32–48.

Jackson CA, Hickey TL. 1985. Use of ferrets in studies of the visual system. Lab Anim Sci 35:211–215.

Kageyama GH, Wong-Riley MT. 1984. The histochemical localization of cytochrome oxidase in the retina and lateral geniculate nucleus of the ferret, cat, and monkey, with particular reference to retinal mosaics and ON/OFF-center visual channels. J Neurosci 4:2445–2459.

Kolb H, Nelson R, Mariani A. 1981. Amacrine cells, bipolar cells and ganglion cells of the cat retina: a Golgi study. Vis Res 21:1081–1114.

Kolb H, Linberg KA, Fisher SK. 1992. Neurons of the human retina: a Golgi study. J Comp Neurol 318:147–187.

Kong JH, Fish DR, Rockhill RL, Masland RH. 2005. Diversity of ganglion cells in the mouse retina: unsupervised morphological classification and its limits. J Comp Neurol 489:293–310.

Leventhal AG, Keens J, Törk I. 1980. The afferent ganglion cells and cortical projections of the retinal recipient zone (RRZ) of the cat's 'pulvinar complex'. J Comp Neurol 194:535–554.

Leventhal AG, Rodieck RW, Dreher B. 1981. Retinal ganglion cell classes in the Old World monkey: morphology and central projections. Science 213:1139–1142.

Lohmann C, Wong RO. 2001. Cell-type specific dendritic contacts between retinal ganglion cells during development. J Neurobiol 48:150–162.

Maslim J, Stone J. 1986. Synaptogenesis in the retina of the cat. Brain Res 373:35–48.

Maslim J, Stone J. 1988. Time course of stratification of the dendritic fields of ganglion cells in the retina of the cat. Brain Res Dev Brain Res 44:87–93.

McGuire BA, Stevens JK, Sterling P. 1986. Microcircuitry of beta ganglion cells in cat retina. J Neurosci 6:907–918.

O'Brien BJ, Isayama T, Berson DM. 1999. Light responses of morphologically identified cat ganglion cells. Invest Ophthalmol Vis Sci 40:S815.

O'Brien BJ, Isayama T, Richardson R, Berson DM. 2002. Intrinsic physiological properties of cat retinal ganglion cells. J Physiol 538:787–802.

Oyster CW, Amthor FR, Takahashi ES. 1993. Dendritic architecture of ON-OFF direction-selective ganglion cells in the rabbit retina. Vis Res 33:579–608.

Peichl L. 1989. Alpha and delta ganglion cells in the rat retina. J Comp Neurol 286:120–139.

Peichl L. 1992. Topography of ganglion cells in the dog and wolf retina. J Comp Neurol 324:603–620.

Peichl L, Buhl EH, Boycott BB. 1987a. Alpha ganglion cells in the rabbit retina. J Comp Neurol 263:25–41.

Peichl L, Ott H, Boycott BB. 1987b. Alpha ganglion cells in mammalian retinae. Proc R Soc Lond B Biol Sci 231:169–197.

Penn AA, Wong RO, Shatz CJ. 1994. Neuronal coupling in the developing mammalian retina. J Neurosci 14:3805–3815.

Penn AA, Riquelme PA, Feller MB, Shatz CJ. 1998. Competition in retinogeniculate patterning driven by spontaneous activity. Science 279: 2108–2112.

Price DJ, Morgan JE. 1987. Spatial properties of neurones in the lateral geniculate nucleus of the pigmented ferret. Exp Brain Res 68:28–36.

Pu M, Berson DM. 1992. A method for reliable and permanent intracellular staining of retinal ganglion cells. J Neurosci Methods 41:45–51.

Pu M, Berson DM, Pan T. 1994. Structure and function of retinal ganglion cells innervating the cat's geniculate wing: an in vitro study. J Neurosci 14:4338–4358.

Reese BE, Urich JL. 1994. Does early enucleation affect the decussation pattern of alpha cells in the ferret? Vis Neurosci 11:447–454.

Rodieck RW, Brening RK. 1983. Retinal ganglion cells: properties, types, genera, pathways and trans-species comparisons. Brain Behav Evol 23:121–164.

Rodieck RW, Watanabe M. 1993. Survey of the morphology of macaque retinal ganglion cells that project to the pretectum, superior colliculus, and parvicellular laminae of the lateral geniculate nucleus. J Comp Neurol 338:289–303.

Rodieck RW, Binmoeller KF, Dineen J. 1985. Parasol and midget ganglion cells of the human retina. J Comp Neurol 233:115–132.

Rowe MH, Stone J. 1977. Naming of neurones. Classification and naming of cat retinal ganglion cells. Brain Behav Evol 14:185–216.

Stein JJ, Johnson SA, Berson DM. 1996. Distribution and coverage of beta cells in the cat retina. J Comp Neurol 372:597–617.

Stellwagen D, Shatz CJ. 2002. An instructive role for retinal waves in the development of retinogeniculate connectivity. Neuron 33:357–367.

Stone J. 1983. Parallel processing in the visual system: the classification of retinal ganglion cells and its impact on the neurobiology of vision. New York: Plenum Press. xvi, 438 p.

Sun W, Li N, He S. 2002a. Large-scale morophological survey of rat retinal ganglion cells. Vis Neurosci 19:483–493.

Sun W, Li N, He S. 2002b. Large-scale morphological survey of mouse retinal ganglion cells. J Comp Neurol 451:115–126.

Troy JB, Schweitzer-Tong DE, Enroth-Cugell C. 1995. Receptive-field properties of Q retinal ganglion cells of the cat. Vis Neurosci 12:285–300.

van Wyk M, Taylor WR, Vaney DI. 2006. Local edge detectors: a substrate for fine spatial vision at low temporal frequencies in rabbit retina. J Neurosci 26:13250–13263.

Vaney DI. 1994. Territorial organization of direction-selective ganglion cells in rabbit retina. J Neurosci 14:6301–6316.

Vitek DJ, Schall JD, Leventhal AG. 1985. Morphology, central projections, and dendritic field orientation of retinal ganglion cells in the ferret. J Comp Neurol 241:1–11.

Wässle H, Boycott BB. 1991. Functional architecture of the mammalian retina. Physiol Rev 71:447–480.

Wässle H, Levick WR, Cleland BG. 1975. The distribution of the alpha type of ganglion cells in the cat's retina. J Comp Neurol 159:419–438.

Wässle H, Voigt T, Patel B. 1987. Morphological and immunocytochemical identification of indoleamine-accumulating neurons in the cat retina. J Neurosci 7:1574–1585.

Watanabe M, Rodieck RW. 1989. Parasol and midget ganglion cells of the primate retina. J Comp Neurol 289:434–454.

Watanabe M, Fukuda Y, Hsiao CF, Ito H. 1985. Electron microscopic analysis of amacrine and bipolar cell inputs on Y- , X-, and W-cells in the cat retina. Brain Res 358:229–240.

Weber AJ, McCall MA, Stanford LR. 1991. Synaptic inputs to physiologically identified retinal X-cells in the cat. J Comp Neurol 314:350–366.

Weidman TA, Greiner JV. 1984. Histology of the ferret retina. Anat Anz 157:329–341.

Wingate RJ, Thompson ID. 1995. Axonal target choice and dendritic development of ferret beta retinal ganglion cells. Eur J Neurosci 7:723–731.

Wingate RJ, Fitzgibbon T, Thompson ID. 1992. Lucifer yellow, retrograde tracers, and fractal analysis characterise adult ferret retinal ganglion cells. J Comp Neurol 323:449–474.

Wong RO, Hughes A. 1987. The morphology, number, and distribution of a large population of confirmed displaced amacrine cells in the adult cat retina. J Comp Neurol 255:159–177.

Yang G, Masland RH. 1992. Direct visualization of the dendritic and receptive fields of directionally selective retinal ganglion cells. Science 258:1949–1952.

Yang G, Masland RH. 1994. Receptive fields and dendritic structure of directionally selective retinal ganglion cells. J Neurosci 14:5267–5280.